energies

MDPI

Review

Hydrothermal Carbonization: Modeling, Final Properties Design and Applications: A Review

Silvia Román [1,*], Judy Libra [2], Nicole Berge [3], Eduardo Sabio [1], Kyoung Ro [4], Liang Li [3], Beatriz Ledesma [1], Andrés Álvarez [1] and Sunyoung Bae [5]

1 Department of Applied Physics, University of Extremadura, Avda. Elvas, s/n, 06006 Badajoz, Spain; esabio@unex.es (E.S.); beatrizlc@unex.es (B.L.); andalvarez@unex.es (A.Á.)
2 Leibniz Institute for Agricultural Engineering and Bioeconomy, Max-Eyth-Allee 100, 14469 Potsdam-Bornim, Germany; jlibra@atb-potsdam.de
3 Department of Civil and Environmental Engineering, University of South Carolina, 300 Main Street, Columbia, SC 29208, USA; berge@engr.sc.edu (N.B.); li286@email.sc.edu (L.L.)
4 USDA-ARS Coastal Plains Soil, Water, and Plant Research Center, 2611 West Lucas Street, Florence, SC 29501, USA; kyoung.ro@ars.usda.gov
5 Department of Chemistry, Seoul Women's University, 621 Hwarang-ro, Nowon-gu, Seoul 01797, Korea; sbae@swu.ac.kr
* Correspondence: sroman@unex.es; Tel.: +34-627-965-005

Received: 3 January 2018; Accepted: 12 January 2018; Published: 16 January 2018

Abstract: Active research on biomass hydrothermal carbonization (HTC) continues to demonstrate its advantages over other thermochemical processes, in particular the interesting benefits that are associated with carbonaceous solid products, called hydrochar (HC). The areas of applications of HC range from biofuel to doped porous material for adsorption, energy storage, and catalysis. At the same time, intensive research has been aimed at better elucidating the process mechanisms and kinetics, and how the experimental variables (temperature, time, biomass load, feedstock composition, as well as their interactions) affect the distribution between phases and their composition. This review provides an analysis of the state of the art on HTC, mainly with regard to the effect of variables on the process, the associated kinetics, and the characteristics of the solid phase (HC), as well as some of the more studied applications so far. The focus is on research made over the last five years on these topics.

Keywords: hydrochar; process modeling; reaction kinetics

1. Introduction

The increasing demand for energy and the rapid depletion of fossil fuels, their non-centralized use as fuel and as raw material in manufacturing with the related consequences for climate change, water contamination, etc., make it imperative to find not only renewable energy sources, but also more sustainable manufacturing methods.

Biomass offers an attractive alternative as a source for biofuels or added-value products for many reasons. Apart from being renewable, it produces low net CO_2 emissions coupled with lower sulfur content. Furthermore, it possesses economic potential under the scenario in which the price of petroleum fuels rise in near future. Ample supplies can also be produced in many countries, thus decreasing energy dependence relations which unfortunately may results in geopolitical conflicts.

In 2014, the world Total Primary Energy Supply (TPES) was 13,700 Mtoe, of which 13.8%, or 1894 Mtoe (up 2.6% in 2013), was produced from renewable energy sources. Breaking this down further shows that 73.2% was due to biofuels and waste (10.1% share of the total energy supply) (Key renewable trends, 2016 IEA Statistics). Even so, the average annual growth rate of biofuels is much lower than that

of solar photovoltaic or wind energy. In particular, solid biofuels (biomass and char) show a very low annual growth rate (1.5%) as compared to other biomass fuels (biogas: 13.2%; liquid biofuels: 10.4%).

Many thermochemical processes can be used to transform biomass into energy (combustion), fuels, and other materials (pyrolysis, gasification, biochemical methods, activation processes...). These processes usually require particular feedstock conditions (e.g., low moisture content, high carbon density, or low ash content) or can be costly and/or involve the use of harmful and/or non-sustainable chemicals (frequently derived from fossil fuels). In such cases, even though the process involves the use of a biomass, its sustainability can be called into question.

Against this backdrop, the preceding decades have witnessed a renaissance in research on hydrothermal processes, and, in particular, on hydrothermal carbonization (HTC), which is being actively studied all over the world. In this process, the feedstock is introduced into water under mild temperature (usually in the range 180–250 °C) and pressure (generally autogeneous) conditions. As the reaction proceeds, biomass is transformed into a char (HC) via combination reactions such as hydrolysis, dehydration, decarbonylation, decarboxylation, polymerization, re-condensation, etc. One of the main advantages of HTC over other thermochemical processes is that prior costly drying processes are not required; in fact, in HTC, residual moisture often plays a dual role, both as solvent and as catalyst [1]. Other additional highlights are related to high solid yields, final product quality (calorific value, ash composition, tunable surface functionalities, presence of natural binders, conductive behavior), ease of operation, low cost, or process energy efficiency [2–6].

We strongly believe that the research on efficient biomass conversion methodologies, such as HTC, can help to encourage a greater use of biomass, and, in particular, of HCs as biofuels and also as carbon materials for other applications. In this latter case, HTC has the potential to provide specific chemical and/or structural characteristics depending on the targeted application. Despite other reviews on HTC have been already published, this one offers a wide perspective, and does not only focus on particular applications that are related to the HC surface properties or the use as biofuel; this review offers an overview of the state of the art in recent research on HTC, focusing on two different perspectives:

(a) Process knowledge, including how experimental parameters can affect the reactions taking place during HTC and final characteristics of the obtained HCs, as well as the reaction kinetics. Both experimental and modeling studies have been reviewed. To the authors' knowledge, no previous HTC reviews have addressed the study of the models associated to the process itself, and this is a strong point of this review.
(b) Applications of HCs, as biofuels in thermochemical processes, adsorbents in liquid solutions, material for electrode in supercondensers, and catalysts.

2. HTC Modeling

2.1. Kinetics Models

Despite the increasing research on HTC and its effectiveness in yielding functional materials, the mechanisms and kinetics involved in the process are not fully understood. The wide variety of phenomena taking place during HTC make the analysis of the process difficult, and only a few attempts have been carried out in this aspect, being mostly focused on HTC of pure materials instead of heterogeneous biomasses. Moreover, most of the studies on HTC kinetics have been limited to the liquid phase, while research on the evolution of the solid phase during the process is relatively scarce. However, progress in developing models capable of describing the kinetics and the governing mechanisms is very important in order to design the equipment and operating conditions that are required to produce char with desired characteristics. In this context, several benefits are expected from the development of a generic model of HTC:

- increased model application for full-scale plant design, operation and optimization;
- common basis for further model development and validation studies to make outcomes more comparable and compatible; and,

- assisting technology transfer from research to industry.

Many of the above points relate to practical, industrial applications. Indeed, this is one of the areas where most benefits from the application of a generic process model can be gained. Most of mathematical models on biomass HTC kinetics have been developed in recent years, but there is room for improving modeling because the development of a generic model for HTC still seems to be far. The objective of this section is to review the current research on modeling HTC kinetics. This information could serve as a starting point for further improvements that are focused on the development of a generic model describing the kinetics of HTC.

The mathematical HTC models can be divided into three categories, namely, basic kinetic models, statistical models, and computational models. The advantages and limitations of them are summarized in Table 1.

Table 1. Advantages and limitations of hydrothermal carbonization (HTC) kinetics models.

Model Category	Advantages	Limitations
Basic kinetic models	• Easy to implement	• Oversimplify the dynamics of rate-limiting steps • Cannot provide enough knowledge for full-scale facilities
Statistical models	• Qualitative and quantitative analysis of the effect of processing parameters on the HTC kinetics	• Are rmpirical models • Their application is restricted to similar feedstock and experimental conditions • Cannot provide enough knowledge for full-scale facilities
Computational models	• Full descriptions of the variations in both time and space • Combine chemical reaction kinetics and physical laws to produced accurate simulation of full-scale applications • Effective and intuitive visual results analysis	• Complex numerical simulation

There is some overlap between these categories as the mass balance for specific state variables is the basis of all mathematical models. The statistical models are empirical models, that is to say, they are based on direct observation, measurement, and extensive data records that allow us to predict the behavior of the system with no understanding of the mechanisms taking place. In contrast, the computational models based on the laws of physics are mechanistic ones because they try to explain the HTC process, analyzing how the experimental conditions affect the chemical reactions, as well as the transfer of mass, heat, and momentum.

2.1.1. Basic Kinetic Models

Most of the reported kinetic models for HTC biomass processes are dimensionless models (0D) that analyze the kinetics of the process by means of a simple analytical expression. The most of them describe the reaction rate as a first-order reaction defined by the Arrhenius equation [7], which strictly should be written as:

$$r = -\frac{dm}{dt} = k(t) \times m = A_0 \times \exp\left(\frac{-E_a}{R \times T(t)}\right) \times m \quad (1)$$

where: $k(t)$ stands for the reaction rate coefficient (time^{-1} units, generally s^{-1}, min^{-1} or h^{-1}) at time t, A_0 is the pre-exponential factor (time^{-1} units, in agreement with $k(t)$), E_a is activation energy (J·mol^{-1}), m represents the mass of solid in the reactor (mass units), R is the universal gas constant

(8.314 J·mol^{-1}·K^{-1}), t is the reaction time (time units, in agreement with $k(t)$), and $T(t)$ represents the temperature (K) at time t.

As Equation (1) is a differential equation with respect to time, its mathematical handling is complex. The common procedure to simplify its use is to consider that the reaction temperature remains constant during the experiment. With this assumption, the differential equation can be easily solved by a separation of variables. Thus, the conversion as a function of time, $X(t)$, for a given temperature, can be expressed in its integral form as a simple exponential equation:

$$X(t) = \exp(-k \times t) = \exp\left(-A_0 \times \exp\left(\frac{-E_a}{R \times T}\right) \times t\right) \quad (2)$$

Determining $X(t)$ at different temperatures, the activation energy (E_a) and the frequency factor (A_0) can be calculated by fitting the experimental and theoretical results.

Using this model, kinetic parameters of various biomass feedstock have been reported, such as synthetic faeces ($A_0 = 1.5 \times 10^7$ min^{-1}, $E_a = 78$ kJ·mol^{-1}) [7], tannins ($E_a = 91$ kJ·mol^{-1}) [8] and glucose ($A_0 = 7.7 \times 10^8$ s^{-1}, $E_a = 114$ kJ·mol^{-1}) [9].

Other authors used the same technique but also considered more complex reaction mechanisms. For instance, Reza et al. [10] studied the loblolly pine as feedstock material and proposed a kinetic model in which hemicellulose decomposes in a first-order reaction (E_a = 29 kJ·mol^{-1}, $A_0 = 58.6 \times 10^5$ s^{-1}) producing aqueous chemicals and gases, while cellulose is also said to decompose by a first-order reaction (E_a = 77 kJ·mol^{-1}, A_0 = 8.24 × 10^5 s^{-1}), which produces a solid product, aqueous chemicals, and gases.

According to Iryani et al. [11], the kinetics of the sugarcane bagasse HTC could be described as two simultaneous first-order reactions (hydrolysis and dehydration reactions) in Arrhenius form ($E_a = 88.1$ kJ·mol^{-1}, $A_0 = 1.6 \times 10^7$ s^{-1}, and 129.4 kJ·mol^{-1}, $A_0 = 2.9 \times 10^9$ s^{-1}, respectively), in which the solid particle is shrinking following a cylindrical shrinking core model.

Jatzwauck and Schumpe [12] studied the kinetics of HTC of soft rush when considering that the first reaction step was the hydrolytic breakdown of the biomass into its basic components (hemicellulose, cellulose, and lignin) (Reaction (1)). The dissolved intermediate products may undergo further reaction to form solid HC (Reaction (2)) or gaseous and dissolved by-products (Reaction (3)). Reactions (1) and (2) were considered to be first order, whereas a somewhat higher order n was expected for the HC formation because they considered that the later process could be favoured at high concentrations of the intermediate products. This resulted in three kinetic constants for the Arrhenius equation at constant T ($E_a{}^1 = 141$ kJ mol^{-1}, $A_1 = 1.89 \times 10^{14}$ h^{-1}; $E_a{}^2 = 75.0$ kJ mol^{-1}, $A_2 = 1.15 \times 10^7$ (1.59) kg$^{-0.52}$ h^{-1}; and, $E_a{}^3 = 74.3$ kJ mol^{-1}, $A_3 = 1.89 \times 10^7$ h^{-1}). In addition to modelling the HTC kinetics in terms of the three basic biomass components (i.e., hemicellulose, cellulose, and lignin), it will be useful, especially for combustion applications of HC, if the proximate components (i.e., volatile matter, fixed carbon, and ash contents) of the feedstock and HC can be predicted with simple kinetic models, as done by Ro et al. [13] for pyrolyzing animal manures. The proximate components of combustion fuels are commonly used to characterize fuel sources by power industry.

Jung and Kruse [14] used an Arrhenius-type overall kinetic equation to model hydrochar mass yield, carbon, and oxygen content of hydrothermal carbonization experiments. The equation is founded on the coalification model proposed by Ruyter [15], having three adjusting parameters: A, B, and C:

$$A \cdot t^B \cdot \exp\left(\frac{-C}{T}\right) = \frac{O_{feed} - O_t}{O_{feed} - 6} \quad (3)$$

where t is time (s), T is temperature (K), O_{feed} is the oxygen content the oxygen content of the feedstock, O_t the oxygen content after t reaction time, and 6 is the oxygen content of the sub-bituminous coal, which is taken as reference (ca. 6 wt %, daf).

Models based on severity factors have been applied by several authors to describe the kinetics of the HTC of different biomass feedstock. This methodology combines the effect of temperature and time in a single factor that defines overall reaction severity. One of the most used is the classical reactivity factor developed by Abatzoglou et al. [16] to characterize hydrolytic depolymerization processes during wood pulping:

$$R_0 = t \cdot \exp\left[\frac{T - 100}{14.75}\right] \quad (4)$$

where R_0 (also called the reaction ordinate) has units of time (min), t (min) is the residence time, and T (°C) is the processing temperature. This expression assumes that the hydrolytic process involves first-order reactions having an Arrhenius dependence upon temperature. A reference temperature of 100 °C is used. This severity factor equation has been used by other researchers for describing the HTC process as applied to various biomass feedstocks. For example, Gao et al. [17] analysed the effect of water to biomass ratio on the HC yield of HTC of corn stalk and longan shell, and Hoekman et al. [18] studied the HTC of loblolly pine in a continuous, reactive twin-screw extruder. Janga et al. [19] applied a more complex severity model for the prediction of the monosaccharide yield via hydrolysis of different wood by concentrated sulfuric acid. Suwelack et al. [20] applied this severity model to predict the gaseous, liquid, and solid mass yield in the HTC of wheat straw.

The main advantage of all these simplified kinetic models is their easy implementation. However, their application under other experimental conditions and for other process set-ups is somewhat limited because they do not take into account mass, heat, and momentum transfer. Notably, the constant temperature assumption cannot always be applied. In fact, it should be noted that most of the kinetic experiments are carried out on batch conditions. Generally, in these experiments, both water and sample are introduced at room temperature, and then heated. Thus, there is a heat-up period in which temperature increases from the starting condition up to the desired HTC temperature. This heat-up period cannot be dismissed in most cases, so the assumption that the temperature is constant during the experimental run should be applied with caution because constant HTC temperatures are the exception, not the rule. Only in bath micro-reactors and reactors in which sample and water enter at the target temperature, can the application be truly applied. Obviously, the higher the difference between T and $T(t)$ during the reaction, the lesser the results' reliability.

Finally, Gallifuoco et al. [21] have developed new experimental methods to be adopted in the industrial HTC processes. This interesting empirical approach is proposed for modelling the evolution of the process variables during the reaction, particularly the electrical conductivity of the liquid phase, which is correctly described by a simple two-step first order mechanism, regardless of the reaction temperature. They found a high correlation between and the solid phase carbon content and the liquid phase conductivity, and suggested to monitor the industrial process by sampling HC liquid and analysing this property.

2.1.2. Statistical Models

Statistical models emphasize the interrelationship between key parameters. The implementation of a Design of Experiments—Response Surface Methodology (DoE/RSM) approach allows for the importance of each variable to be identified, as well as their interactions, by developing a model with inlet parameters (processing variables) and outlet functions (interest parameters); it can therefore provide information of the effect of experimental conditions on the direction and magnitude of the response measured. In this way, it has a huge potential to study and optimize a wide range of engineering systems and has been often used in energy processes (such as pyrolysis, gasification, transesterification, biodigestion, drying, or pelleting) or applications (different types of fuel cells, batteries, internal engines...) [22]. Moreover, this methodology allows for the design of experiments under particular conditions in order to maximize the information that can be extracted from the results, and, provided the model works and the experimental data fitting is good, it can be used to predict the system behaviour under different conditions.

DoE/RSM methodology has also been used in the analysis of HTC processes. For example, Heilmann et al. [23] studied the importance and interdependence of temperature, time, and % solid on the HTC of microalgae by using a three variable, two-level factorial experiment with replicated center points. A linear regression for the carbon recovered was developed from the orthogonal factorial design (dimensionless variables):

$$\%Carbon\ Recovered = 51.54 - 1.375T - 0.375t + 9.875\%\ solid \quad (5)$$

Álvarez-Murillo et al. [24] or Sabio et al. [25] used this methodology to understand the HTC process of olive stones and tomato peel, respectively, by developing models in which the inlet experimental variables were Solid/Water ratio, processing time, and temperature, and the outputs were solid yield, HHV, H/C, and O/C atomic ratio. The DoE was carried out by using a Central Composite Design (CCD). This procedure involves the use of a two-level factorial design with $2k$ points combined with $2k$ axial points and n center runs (tests were made at central location; 0, 0, 0), with k being the number of factors. With k factors, the total number of experiments, N, is

$$N = 2^k + 2k + n \quad (6)$$

CCD is useful in RSM because it provides an even distribution of the experimental points, which improves the accuracy of the further fitting. Álvarez-Murillo and Sabio et al. [24,25] applied a 2nd order model to describe the change of solid yield (SY) as a function of the processing dimensionless variables:

$$SY_{stone} = 43.6 + 3.44R - 5.56T - 3.24t + 3.27RT - 0.814Rt + 1.42Tt - 1.62R^2 + 1.10T^2 + 2.53t^2 \quad (7)$$

$$SY_{peel} = 61.9 + 3.22R - 10.2T - 9.25t + 2.05RT - 0.94Rt - 4.79Tt - 2.79R^2 - 5.78T^2 + 1.50t^2 \quad (8)$$

where R represents the solid/liquid ratio (-), T the reaction temperature, and t the reaction time. These authors concluded that increases in both temperature and residence time markedly reduce the SY, increasing energy densification. Danso et al. [26] used a CCD for studying the hydrothermal carbonization of primary sewage sludge. The effect of temperature and reaction time on the characteristics of solid (hydrochar), liquid and gas products, and the conditions leading to optimal hydrochar characteristics were investigated, obtaining the following equation for the solid yield:

$$SY(\%) = 11.49 - 0.26T - 3.24t \quad (9)$$

Kannan et al. [27] also used a CCD for guiding the optimization of microwave hydrothermal carbonization (MHTC) of the industry fish waste, finding the following equation for the solid yield:

$$SY(\%) = -377.1 - 4.1662T + 0.6413t - 0.00031Tt - 1.62R^2 - 0.0110T^2 - 0.0102t^2 \quad (10)$$

An advantage of the DoE/RSM procedure is that the fitting equations may be depicted graphically to improve visual information about the kinetics as a function of the processing variables, allowing for to obtain better understanding of the local analysis. Figure S1, supplied as supplementary material and taken from reference [25] shows the strong interaction of variables during HTC of tomato waste. Makela et al. [28] used response-surface contour plots to show the effect of HCl or NaOH on the HTC of sludge from a pulp and paper mill. The result show that the pattern solid yield as a function of temperature and time is not affected by the addition of acid or base.

2.1.3. Computational Models

As it has been explained previously, a general practice in the study of HTC reaction is to apply dimensionless models (no influence of the spatial variables; the system behaves in the same way in any point of the reactor), with the assumption that the reaction temperature is constant

during the whole experiment. Both assumptions (0D system and $T(t) = T$) should be applied with caution because temperature is a function of time and space ($T(t, x, y, z)$), so the validity of them depends on the experimental conditions (type of reactor, size, stirring, heating rate, etc.). In this context, three-dimensional (3D) computational models offer a versatile approach to study not only the kinetics of the HTC process but also the mass, temperature, and velocity fields, turbulence, particle trajectories, rates of energy dissipation, transport of dissolved components, and to determine volumes of high mixing intensity and stagnant zones, based on reactor geometry, feed locations, and operating conditions. These models provide an accurate picture of the processes taking place in the reactor and allow for us to verify the validity of dimensionless and constant temperature assumption. Computational models can be implemented by the following procedures: (1) constructing the geometry of the reactor studied in a computer aided design type program; (2) fitting a mesh to divide up the entire domain into smaller cells; (3) setting boundary conditions (such as inlets, outlets, and walls) and initial conditions (4) defining the properties of different phases (gas, liquid and solids); and (5) selecting different solvers and turbulence models to calculate how the phase/phases are affected by the geometry and boundary conditions in each individual cell defined by the mesh.

Once validated, the computing model can be used to design, evaluate, and optimize the HTC process. Álvarez-Murillo et al. [29] applied the computational model to investigate the kinetics of cellulose hydrothermal carbonization over different reactions times and temperatures, verifying that the system behaves like a 0D system and developing a first order-reaction model based on the Arrhenius equation, in which temperature is a function of time, $T(t)$ (K):

$$r = -\frac{dm_{cell}}{dt} = 2.46 \cdot T(t)^{2.2} \cdot \exp\left(\frac{-90,100}{8.314 \cdot T(t)}\right) \quad (11)$$

To determine $T(t)$, the model resolves simultaneously mass, heat, and momentum transfer. Figure 1 summarizes how the model works: the fluid velocity and temperature fields are determinant in the whole experimental domain, and with this information the kinetics of every component is determined in each point of the reactor. According to the model, mass species evolutions are described by sigmoid curves and the presence of an induction period confirms the importance of taking into account the heat-up time and not only the T-constant period during the experiments. Moreover, the model indicates that temperature plays a main role in the cellulose HTC reaction, affecting both pre-exponential and exponential factors of the kinetic constant.

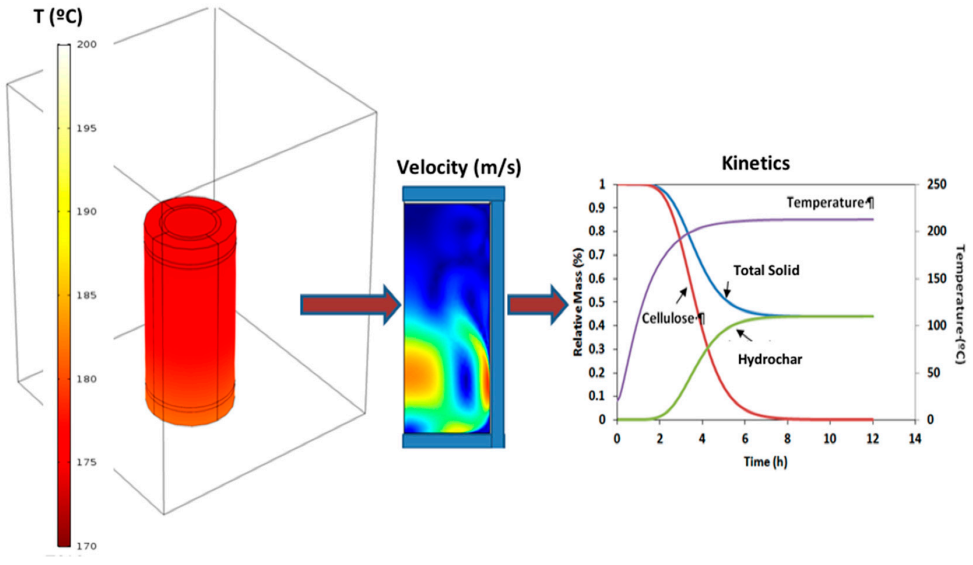

Figure 1. Computational model summary.

2.2. Hydrochar Properties

A large body of literature that is associated with the hydrothermal carbonization of various organics over a range of process conditions exists (see Tables S1 and S2, provided as supplementary material). Approximately 71% and 54% of the papers that describe HC-related properties report HC yield and HC carbon content, respectively. HC properties are dependent on both process conditions (e.g., reaction time, temperature) and feedstock properties (e.g., carbon content). Understanding and accounting for these interactions is important when developing models to predict HC properties.

2.2.1. Influence of Process Conditions on HC Properties

Reported results from HTC studies that were conducted over a range of process conditions have been surveyed to ascertain how carbonization process conditions (e.g., reaction time and temperature and initial biomass concentration) influence HC properties. Previous reviews on HTC have given evidence about the effect of experimental conditions [1,30]; in this work, we provide updated information based on research conducted during last five years. Table S1 provides an updated review on the trends reported since 2010), while Table S3 collects information about the influence of process parameters on HTC.

Changes in temperature have been shown to influence HC chemical characteristics and morphology [31], HC energy content [4,32–35], and liquid-phase organic concentrations [36,37].

Generally, as reaction temperatures increase, solid yields decrease [2,5,31,38]. This likely occurs because the extent of feedstock hydrolysis and dehydration increases with reaction temperature, and because enhanced temperature also increases the potential for compound volatilization and dissolution. This is consistent with reports that temperature influences liquid-phase carbon content, with higher reaction temperatures resulting in greater initial feedstock solubilization, and thus lower solid-phase carbon [36]. The carbon content of the solids has been reported to increase as reaction temperatures increase [1,31,39], also resulting from feedstock dehydration. The oxygen content of the feedstock has also been shown to decrease with increasing reaction temperature; this phenomena has been reported as the most significant contribution to the declining trend of recoverable solids [36,39] and increasing energy content at higher temperatures [4,35]. Reaction temperature has also been shown to influence carbonization rates, with higher temperatures being correlated with the accelerating of carbonization reactions [36].

Reaction time, although studied in less detail than reaction temperature, has also been shown to influence carbonization product characteristics. At short reaction times, Lu et al. [36] report that significant fractions of the feedstock are solubilized, with HC formation subsequently increasing over time and leveling off to a maximum level. Reaction time has also been shown to influence carbon distribution [9,32,36,40,41], and HC chemical characteristics and energy content [36,39–41]. Solids yields have been shown to decrease with reaction time [24,36,40–43], while the carbon and energy contents of the solids has been shown to increase with time [36,39–41]. The analysis of HTC time effect in studies in which the interaction of variables was considered has demonstrated that the effect of this parameter significantly depended on biomass load [24,25,42]. Others have reported that reaction time does not have a significant impact on carbonization product formation/characteristics [4,24,43], which may be an artifact of the process conditions investigated; if carbonization data were collected following complete conversion of the feedstock (i.e., state at which the feedstock is no longer being converted), then reaction time will likely not be important. In addition, the defining of reaction time is not uniform. In some studies, reaction time is referred to as the time following reactor heating [32,44–46], while in other studies, reactor heating is included [2,40,41]. When evaluating carbonization data to understand the influence of reaction time, it is critical to ascertain whether the reported data represent points prior to or following complete feedstock conversion. Thus, it is recommended that the reaction time necessary to reach stabilized carbonization products be routinely reported because such information depends on reaction kinetics and will vary for different feedstock types, reactor volumes, and heating rates. The influence of reaction time on carbonization product

characteristics is also likely to be dependent on reactor heating time (HT) and/or heating rate (HR). However, few studies report heating rate/time information [29].

Initial feedstock concentration has also been reported to influence HC characteristics. Li et al. [40] found that as initial solids concentration decreased (i.e., initial water content increased), the fraction of carbon partitioning to the liquid-phase increases. Changes in initial feedstock concentration have also been reported to influence HC yields [24,41] and carbon distribution [40]. The degree of this influence is also greatly affected by reaction temperature and time. Generally, studies report that as the initial solids concentration increases, solid yields increase [24,25,40].

2.2.2. Influence of Feedstock Properties on HC Characteristics

Changes in feedstock type have been shown to influence HC properties [2,44,47]. There are also reports that indicate changes in feedstock type have little influence on solids characteristics [48–51]. The differences in these observations likely depend on the feedstocks that are being evaluated. Table S4, provided as supplementary material, reviews recent works on the influence of changing feedstocks in HTC studies. Berge et al. [2] report that model food waste results in larger solids yields with larger energy content than that obtained from paper or representative mixed municipal solid waste (MSW). Titirici et al. [52] characterized solids formed when carbonizing a variety of sugars and biomasses. They found that all sugars in their hexose form degrade to hydroxymethylfurfural and then condense to solid carbonaceous materials with similar chemical and structural composition [52]. However, solids that are formed from the carbonization of different pentoses are relatively different from one another [52]. The influence of lignin on the hydrothermal carbonization of several mixed feedstocks has been tested and well documented [1,47,53]. Dinjus et al. [53] carbonized several mixed feedstocks (e.g., straw, grass, cauliflower, beechwood) to understand the influence of lignin on carbonization and reported that lignin presence impedes the carbonization process by ultimately forming a protective shell around such feedstocks. Lu and Berge [47] reported that changes in feedstock properties/complexity influence HC yield and energy content, but do not impart a statistically significant influence on HC carbon content. Lu and Berge [47] also indicated that HC yields increase with an increasing feedstock carbon content and that feedstock complexity influences carbonization kinetics.

Finally, recent studies have reported the influence of HTC experimental conditions on the ash properties of HCs. Improvement of ashes can be significantly important for HCs to be used as fuel, since it can prevent slagging and fouling behavior, as well as corrosion of the process equipment. The work undertaken by Makëla et al. [54] provides a complete analysis on the ash characterization of industrial waste biomass using univariate regression techniques. These authors concluded that the precursor ash content determines the ash yield as well as its chemical composition and solubility; according to these results, two different groups were distinguished: (a) HCs produced from virgin biomass (terrestrial and aquatic) and agricultural, compost or manure biomass; and (b) HCs from higher ash feeds, such as municipal solid waste or sludge from wastewater treatment plants.

2.2.3. Review of Models Developed to Predict HC Properties

Although several models have been developed to predict HC properties, their universal application, with some exceptions, remains untested. Statistic models based on experimentally obtained data have been developed to predict HC properties. A summary of the various statistic models reported in the literature is presented in Table 2.

Table 2. Summary of Statistically Based Models Predicting Hydrochar Properties.

Hydrochar Property	Modeling Approach	Description of Data Used in Model			Reference
		Feedstock	Process Conditions	Data Points	
Hydrochar Yield	Linear regression	Data was collected from the literature, various feedstocks were used	Data was collected from the literature, various conditions were included	263	[55]
	Regression tree	Data was collected from the literature, various feedstocks were used	Data was collected from the literature, various conditions were included	263	[55]
	Quadratic model	Olive stones	Biomass/water ratio: 1.1–12.3%; Temp: 150–250 °C; Time: 3.2–36.8 h	18 experiments, designed using response surface methodology	[24]
	Quadratic model	Shrimp waste	Temp: 150–210 °C; Time: 1–2 h	13 experiments, designed using response surface methodology	[56]
	Linear regression	Anaerobically digested maize silage	Biomass Conc.: 42.3 g/L; pH: 3–7; Temp: 190–270 °C; Time: 2–10 h	15 experiments, designed using Box-Behnken fractional design	[46]
	Quadratic model	Palm shell	Biomass/water ratio: 1.10–1.60; Temp: 180–260 °C; Time: 0.5–2 h	20 experiments, designed using response surface methodology	[57]
	Quadratic model	Tomato-peel waste	Biomass/water ratio: 3.3–12.3%; Temp: 150–250 °C; Time: 1.6–18.4 h	18 experiments, designed using response surface methodology	[25]
Hydrochar carbon content	Linear regression	Data was collected from the literature, various feedstocks were used	Data was collected from the literature, various conditions were included	248	[55]
	Regression tree	Data was collected from the literature, various feedstocks were used	Data was collected from the literature, various conditions were included	248	[55]
	Linear regression	Anaerobically digested maize silage	Biomass Conc.: 42.3 g/L; pH: 3–7; Temp: 190–270 °C; Time: 2–10 h	15 experiments, designed using Box-Behnken fractional design	[46]
Carbon yield (g C/g dry feedstock)	Linear regression	Data was collected from the literature, various feedstocks were used	Data was collected from the literature, various conditions were included	244	[55]
	Regression tree	Data was collected from the literature, various feedstocks were used	Data was collected from the literature, various conditions were included	244	[55]
Energy content	Linear regression	Data was collected from the literature, various feedstocks were used	Data was collected from the literature, various conditions were included	220	[55]
	Regression tree	Data was collected from the literature, various feedstocks were used	Data was collected from the literature, various conditions were included	220	[55]
	Quadratic model	Olive stones	Biomass/water ratio: 1.1–12.3%; Temp: 150–250 °C; Time: 3.2–36.8 h	18 experiments, designed using response surface methodology	[24]
	Quadratic model	Shrimp waste	Temp: 150–210 °C; Time: 1–2 h	13 experiments, designed using response surface methodology	[56]
	Quadratic model	Tomato-peel waste	Biomass/water ratio: 3.3–12.3%; Temp: 150–250 °C; Time: 1.6–18.4 h	18 experiments, designed using response surface methodology	[25]

The relationship between process conditions (e.g., reaction time and temperature and initial solids concentration) and HC yield and energy content are most often investigated. The majority of these relationships are based on data associated with each individual study, often based on second-order data fits resulting from the use of design of experiment approaches, such as response surface methodology. Because these models are based on specific feedstock and narrow process conditions, the universal application of such models is limited. The linear and non-linear regression models developed by Li et al. [55] are an exception to this. These regression models are based on data fits that are associated with the literature-collected hydrothermal carbonization information and are thus based on a range of different feedstock properties and process conditions. Leave one out cross-validation of these regression models was conducted to evaluate their ability to predict HC properties. Results from this process indicate that the models can be used to reasonably predict HC properties, generally indicating the non-linear regression tree approach predicts HC properties equivalent to or better than the linear models. Li et al. [55] also report that based on results from this regression analysis, process conditions are more influential on HC yields, while feedstock properties are more influential on the HC carbon content, energy content, and normalized carbon content of the solid.

Other modeling approaches have also been used to predict HC properties. Several kinetic models have been developed that are comprised of a series of first-order reactions used to describe the HTC process [7,9,10,12,29] and ultimately used to predict HC properties (e.g., yield, carbon content). Calibration and determination of the kinetic constants in these models are based on experimental data associated with each individual study. Iryani et al. [11] described the development of a shrinking core model that was ultimately used to describe the hydrolysis process and HC yields. Suwelack et al. [20], and Guo et al. [58] modeled HC properties based on process severity factors. Suwelack et al. [20] developed a model to predict HC yields, degree of carbonization, and H/C and O/C ratios resulting from the HTC of digestate and wheat straw based on the logarithmic dependence on process severity, which was calculated based on batch experiment data. Guo et al. [58] developed models to predict HC yield, carbon content, and energy content using process severity and a dose-response function for data from the carbonization of corn stalk, longan shell, NaOH-pretreated longan shell, wood, olive stone, and grape marc. Based on model results, Guo et al. [58] report that the water to biomass ratio significantly influences HC yield and that feedstock chemical composition has a significant effect on the HC yield, carbon content, and energy content. No cross-validation or testing of the ability of these models to predict HC properties resulting from the carbonization of feedstocks and/or process conditions other than those in which the models are based has been reported.

3. Applications

HTC has proven to be a powerful method to synthesize a wide variety of carbon materials. Titirici et al. [59] made a review on it, which was mainly focused on the chemical structure of these materials, including carbon microspheres, carbon nanofibers or aerogels, mainly obtained from pure biomass (glucose, starch, lignin). Their work also addressed applications that were related to the existence of particular surface functionalities of these materials, which can be tuned up by including modifications to HTC process, such as the addition of nanoparticles, chemicals, or coatings. In our work, we only consider pieces of research on HTC of heterogeneous biomass and devoted to the production of granular HCs.

3.1. Biofuel

As previously described, HTC possesses extensive potential for producing high energy-density solid fuels. First, the high heating value of HCs makes them competitive to other carbon forms, such as lignite [55]. Secondly, because of other advantageous features, such as tunable ash or sulphur and nitrogen content [60], the presence of natural binders which might facilitate further pelleting [6], and lower slagging and fouling indices that make it more favorable for combustion [61]. The behavior of HCs in combustion and gasification processes has been tested under a variety of conditions and scales, and is reviewed below.

The combustion behavior of HCs has been mainly studied at laboratory scale and mostly by means of thermogravimetric analyses (TGA). Also, several authors have successfully investigated co-combustion processes (HC plus coal) as a flexible mechanism to adjust fuel properties (ignition, peak temperature, heat loss, emissions ...) for optimal operation conditions. He et al. [60] reported the behavior of HCs from sewage sludge, coal, and their mixtures during combustion by TGA. Despite presenting dissimilar thermal events that are associated to their different compositions; the authors concluded HCs and their blends with coal could be efficiently used in existing co-firing power plants. NO_x gas emissions also decreased as a result of blending, as well as the formation of corrosive H_2SO_4.

From an industrial point of view, the combustion behavior must be observed, paying attention to the operating conditions, and this includes the ash behavior. The ash content in the fuel could lead to several issues in the boiler, fouling, slagging effect, or even ash melting are the most common. Li et al. [55] studied the effect of HTC on the combustion characteristics of paper sludge and found that including HTC as a pretreatment dramatically improved the combustion slagging and fouling problems; in addition, chlorine content concentration was decreased, allowing for the boiler to be operated under better conditions, and therefore yielding a better combustion performance.

The integration of the HTC technique in a traditional cogeneration power plant (CHP) has been preliminary studied by Saari et al. [62]. They presented a scenario evaluated in terms of the energetic and economic parameters to obtain a profitable project for producing HCs with the heat of a combustion plant. The results indicate that the integration of the HTC plant could offer a better economic liability when compared to the stand alone CHP for a district heating, however, they detected some weaknesses in the HTC market, as well as in the operation and maintenance of an HTC facility. In spite of this purposeful integration, some drawbacks such as the use of a high amount of water, and the treatment of the liquid effluents, which would increase the exploitation cost, should also be considered. Some potential alternatives are the use of the process liquor as a source of high valuable organic compound, such as levulinic acid, hydroxymethylfurfural, phenols, etc., or alternatives, such as treatments in a sewage plant for methanization purposes. Moreover, the production of the liquid fraction can be promoted, and its composition tuned up to favor the production of particular compounds. Some authors have recently studied this fraction in terms of the valuable liquids originated from biomass hydrothermal processes, suggesting a high commercial rentability [63].

HCs have also been tested as precursors to produce syn-gas (or, in general, a gas with a calorific value adequate for energetic purposes) by means of gasification processes with air or steam as gasifying agents. Owing to its greater carbon content as compared to the respective precursors, HCs can provide a greater proportion of CO and H_2 (and under certain circumstances, of CH_4). In addition, the gas composition and flow rate is less variable over time, owing to the lower volatile matter of HCs. Álvarez-Murillo et al. [24] and Moon et al. [64] found similar results using olive stone and sewage sludge, respectively. On the other hand, Lin et al. [65] found that HTC as a pretreatment improved the CO_2 gasification of municipal solid wastes (MSW), promoting a higher reactivity. Furthermore, Gunarathne et al. [66] accomplished a study in a continuous updraft gasifier located in a pilot plant, gasifying HC from spent grains from a brewery. Despite their promising results (syn-gas with a calorific value of 7.9 $MJ \cdot Nm^{-3}$), the authors found some problems due to ash slagging, which suggests that special attention should be paid to these phenomena, as is also the case with combustion experiments.

3.2. Adsorbent

A promising application for the HTC process is to produce new sorbents for environmental applications to prevent unwanted transport of compounds between environmental compartments [67]. This can be between soil-water interfaces, such as agricultural field and water bodies, or between water-water interfaces, such as water bodies and drinking water supply systems, or wastewater systems and natural waterways. Adsorption, especially for drinking water purification purposes, is currently one of the most important traditional application fields for pyrochars. Most of the chars that are used in such systems are produced from single biomass types via pyrolysis and often activated. With the

heightened interest in utilizing locally available, low-cost organic residues, the spectrum of possible feedstocks for sorbents has greatly expanded [68]. Especially with the push to find more sustainable pathways for wet agricultural residues and decrease their environmental impact, more non-traditional chars often with high mineral content are being produced via the HTC-process and evaluated for their adsorption capacities. It may be possible to utilize both the organic as well as mineral content in the chars to remove contaminants [69]. Their potential as a precursor material for the production of activated carbon is also being tested.

Feedstocks for HCs that have been tested for their sorption ability range from woody landscape/forestry residues (sawdust [69]; bamboo sawdust [70]), bioenergy crops (switchgrass [71]) agricultural residues (animal manures [72,73]; wheat straw and corn stalk [69]) to food processing (rice husks [74]; penaut husks [75]; banana peels [76]; orange waste, olive pomace, compost [74]) and domestic wastewater sludges (digested sewage sludge [77]; faecal sludge [78]).

The environmentally relevant target compounds that have been studied as sorbates span the range from organic agrochemicals, such as pesticides and herbicides (fluridone, norflurazon [79]; isoproturon [80]; atrazine [77]), pharmaceuticals and personal care products (tetracycline [81]; diclofenac, salicylic acid, fluriprofen [82]; triclosan, estrone, acetaminophen, carbamazepine [73]; sulfamethoxazole, carbamazepine, bezafibrate, diclofenac [77]), PAHs, endocrine disrupting chemicals and dyes (phenanthrene [83]; pyrene [72], bisphenol A, 17a-ethinyl estradiol [83]; methylene blue [84–86]; Congo red, 2-napthol [70]) to heavy metals Pb (II), Cu (II), Cd (II), Sb (III), Zn (II), As, and phosphate [69,71,73–75,78,84–87].

With the search for low cost sustainable technologies for providing safe drinking water in developing countries [88] and the implementation of increasingly stringent environmental regulations in industrial countries to protect water bodies from organic and inorganic contaminants [89], there is a need to develop cost-effective adsorbents from residual materials, matching application requirements with local abundance of feedstock and appropriate production technology. Many adsorption studies with non-activated pyrochars have been carried out in the last decade and have been summarized in recent reviews that are focused on contaminant removal from water soil and soil and water. The objective of this section is to review the current research on adsorption with HCs. The focus of the research varies from comparing sorption effects of HCs from different feedstocks ([81,84]), with modification/activation (KOH: [69,71,77,78], H_2O_2: [75]; CO_2: [85]; N_2: [81]), with other materials (PAC: [75], organic matter associated with soils: [79]), to compare HC vs. pyrochars [79], mostly from the same feedstocks [73,74,87].

3.2.1. Sorption Capacities

Heavy Metals

The majority of the sorption isotherm experiments with HC and heavy metals found that the Langmuir model fit the isotherms better than the Freundlich model, allowing for q_c to be estimated [69,73,75,76,78], (Table 3). However, a good fit was usually found also with the Freundlich model, resulting in favorable values for 1/n ranging between 0.16 and 0.64. Pellera et al. [74] found linear or Freundlich models fit best for Cu (II) sorption on four hydro- and pyrochars for agricultural residues, while the sorption of Cu (II) and Cd (II) on HC from switchgrass did not fit either of the two isotherm models [71].

Among the studies of single metal adsorption on HC, lead Pb (II) and cadmium Cd (II) were most frequently investigated, followed by copper Cu (II) and antimony Sb (III) (Table 1). The lead sorption studies used plant-based HCs and exhibited a large variation in q_c dependent on feedstock and modification technique. The values ranged from 0.88 mg/g vs. 22.82 mg/g for non-modified peanut hull HC vs. H_2O_2-modified [75] over 45.3 mg/g for micro-wave assisted HC made from Prosopis africana shell [87] to 359 mg/g for HC from dried banana peels made with H_3PO_4 [76]. In contrast, a much narrower range of cadmium sorption capacities was found for plant-based and manure-based HCs and pyrochars (13.9–81.32 mg/g). The values for Cd (II) sorption on manure-derived pyrochars (33.44–81.32 mg/g) ([73]) were significantly higher than those for HCs (13.9–38.3 mg/g) [69,71,73,87],

even with KOH-activation (30.40–40.78 mg/g; [65,67], and plant-derived pyrochars (29.9 mg/g) [87]. A similar behavior for antimony sorption was seen [69]. The process temperature for char production influenced the sorption capacities in the order P250 > P450 > P600 > H250 for both metals (P-pyrolysis, H-HTC). They attributed the higher sorption affinity of manure-derived pyrochar for Cd (II) and Sb (III) to their higher ash content when compared to plant-derived pyrochars, and the dominant mechanism to be cation exchange between the metals and the cations within the ash. The distinct differences in the sorption capacities between the heavy metals on the same sorbent were attributed to the size of the hydrated ionic radii of the metals, where the radii follow the order Cd (II) > Cu (II) > Pb (II) [75–85]. The low sorption affinity of copper and cadmium as compared to lead on the same HCs suggests that they did not bind at all available sites.

Activation of HCs with KOH, however, raised the Cu (II) sorption capacities of faecal sludge and switchgrass HCs significantly up to the range found for Cd (II) (18.6–31 mg/g [71,78]). In general, activation with KOH or modification with H_2O_2 greatly increased the sorption capacities of HCs (3–25 times) [69,71,75,78], although modification had less effect on BET-surface area or even decreased it. Reported N_2-BET-surface areas of HCs and pyrochars ranged from 0.42 to 31.65 m^2/g and show little correlation with their sorption capacities. This is in sharp contrast to the results Fang et al. [85] found with CO_2-activation of two HCs at temperatures up to 900 °C. The sorption rates for methylene blue and lead were strongly positively correlated to the surface area, while copper and cadmium showed weaker trends. However, the high temperature CO_2 activation increased the N_2-SA from 7 to 310–1308 m^2/g, almost three orders of magnitude higher than most of the modified HCs listed in Table 1. Characterization measurements with FTIR showed that both H_2O_2 modification and KOH-activation increased the oxygen-containing functional groups, particularly carboxyl groups, on the HC surfaces [69,71,75,78]. Regmi et al. [71] illustrated the importance of surface composition over surface area in their comparison of switchgrass KOH-activated HC with PAC, which showed little affinity for Cu (II) and Cd (II), even though the PAC had more than two-orders of magnitude greater surface area.

Organics

In contrast to the sorption behavior of heavy metals, the sorption isotherms of organic compounds on hydro- and pyrochars were fit best by the Freundlich model [72,79]. The span of 1/n values for the diverse organic compounds was larger, from highly nonlinear (600 °C pyrochars/estrone 0.22) to approaching linearity (HC/phenanthrene 0.91). Since q_c cannot be determined for compounds with Freundlich isotherms, another method used to compare adsorption behavior of organic compounds is based on the sorption distribution coefficient K_d. The distribution or partitioning of a sorbate between sorbent and water is often found to be linear for low concentrations of organic compounds in natural systems, and K_d is defined as the ratio between q_e and C_e. Furthermore, the sorption of organics has often been found to correlate well with the organic fraction of solids, so K_d can be normalized for the organic carbon content of the sorbent (K_{OC}) and used to compare the relative importance of the other fractions in the system. The log of the OC-normalized distribution coefficient K_{OC} has been used to compare the sorption capacity of various chars for a wide range of hydrophobic organic pollutants [72,79]. The comparison of the logK_{OC} values is made at equivalent sorbate concentrations expressed as a fraction of their water solubility. Some values for sorption of organics with a wide range of hydrophobicity on hydro- and pyrochars are found in Table 4. HCs exhibited higher sorption affinities for organic pollutants with a wide range of hydrophobicity than pyrochars obtained at both low and high temperatures from the same feedstock [72,79]. This was not the case for heavy metal sorption, where HCs showed lower or similar sorption capacities (Table 3). Since HCs exhibited consistently higher logK_{OC} for both nonpolar and polar compounds than pyrochars that were obtained at both low and high temperatures, Han et al. [72], concluded that the dominant amorphous C associated with both alkyl and aryl moieties within HCs explained their high sorption capacity for the organic compounds. The decline in HC aliphaticity after acetone washing, which was coupled with a decrease in the sorption ability of HCs, supports this conclusion.

Table 3. Comparison of sorbent characteristics (maximum sorption capacities q_c, surface area SA) for heavy metals and various hydrochars, modified or activated hydrochars and pyrochars.

Feedstock	Temperature (Time)	SA-N_2	SA-CO_2	pH Optimum	Sorption Capacity q_c (mg/g)					Isotherm Model *	Reference
		(m^2/g)	(m^2/g)	-	Pb (II)	Cu (II)	Cd (II)	Sb (III)	Zn (II)		
Hydrochars											
prosopis africana shell	200 °C (20 min, microwave)	6.05		Pb: 6, Cd: 8	45.3	-	38.3	-		L > F	[87]
sawdust	200 °C (20 h)	4.41		4–8	-		14.5			L > F	[69]
wheat straw	200 °C (20 h)	9.14		4–8	-		13.9			L > F	[69]
corn stalk	200 °C (20 h)	8.58		4–8	-		14.5			L > F	[69]
sawdust (multi-metal)	200 °C (20 h)				3.8	2.2	1.3		0.7	n.r.	[69]
wheat straw (multi-metal)	200 °C (20 h)				2.8	2.2	1.3		0.7	n.r.	[69]
corn stalk (multi-metal)	200 °C (20 h)				2.9	2.7	1.6		1.3	n.r.	[69]
switchgrass	300 °C (30 min)	-				4.0 **	1.5 **				[71]
peanut hulls	300 °C (5 h)	1.3	96.9	-	0.88					L > F	[87]
swine solids	250 °C (4)	1.87	22.38				27.18	3.98		LL > L > F	[73]
poultry litter	250 °C (4)	2.77	24.23				19.8	2.24		LL > L > F	[73]
faecal sludge	200 °C (5 h)	4.03				n.r.					[78]
compost (MSW)	300 °C (30 min)	-	-	5–6		7.72	-	-	-	F > L	[74]
Modified or activated hydrochars											
sawdust	200 °C (20 h) + KOH	0.69					40.78			L > F	[69]
wheat straw	200 °C (20 h) + KOH	0.42					38.75			L > F	[69]
corn stalk	200 °C (20 h) + KOH	1.84					30.4			L > F	[69]
sawdust (multi-metal)	200 °C (20 h) + KOH				15.6	8.9	4.2		3.8	n.r.	[69]
wheat straw (multi-metal)	200 °C (20 h) + KOH				21.8	11.8	4.7		3.6	n.r.	[69]
corn stalk (multi-metal)	200 °C (20 h) + KOH				18.8	10.0	4.6		3.1	n.r.	[69]
peanut hulls	300 °C (5 h) + H_2O_2	1.4	114.4	-	22.82					L > F	[75]
peanut hulls (multi-metal)	300 °C (5 h) + H_2O_2	1.4	114.4	-	16.45	1.22	0.21			ADM	[75]
switchgrass	300 °C (30 min) + KOH	-				31 **	34 **				
banana peels (fresh)	230 °C (2 h/H_3PO_4)	31.65		7	193					L > F	[77]
banana peels (dried)	230 °C (2 h/H_3PO_4)	15.76		7	359					L > F	[77]
faecal sludge	200 °C (5 h) + KOH	4.41				36.63				L > F	[78]
Pyrochars											
prosopis africane shell	350 °C (10 min)	3.11			31.3		29.9	-			[87]
swine solid	250 °C (4 h)	1.2	29.13				81.32	13.09		LL > L > F	[73]
swine solid	450 °C (4 h)	14.25	138.99				76.18	12.66		LL > L > F	[73]
swine solid	600 °C (4 h)	5.51	205.56				33.44	4.44		LL > L > F	[73]
poultry litter	250 °C (4 h)	2.99	35.11				57.69	16.28		LL > L > F	[73]
poultry litter	450 °C (4 h)	4.76	135.74				35.15	8.27		LL > L > F	[73]
poultry litter	600 °C (4 h)	4.2	150.01				33.48	6.63		LL > L > F	[73]
compost (MSW)	300 °C (6 h)			5–6		7.94				F > L	[74]
compost (MSW)	600 °C (6 h)			5–6		3.38				F > L	[74]

* L—Langmuir, F—Freundlich, L-L—Langmuir-Langmuir; ** adsorption density.

Table 4. Comparison of sorbent characteristics (maximum sorption capacities q_c, surface area SA) for some hydrochars (H) and pyrochars (P) and the concentration-dependent distribution coefficients ($\log K_{OC}$) from isotherm experiments with various organic compounds.

Feed-Stock	Process-T (Time)	N_2-SA	CO_2-SA	C_o (mg/L)	Pyrene **	Triclosan **	Estrone **	Carba-Mazepine **	Acetamino-Phen **	Fluridone **	Nor-Flurazon **	Bisphenol A *	17a-Ethinyl Estradiol *	Phenan-Threne *	Reference
					0.001–0.12	0.1–10	0.2–20	0.2–100	0.2–100	n.r.	0.4–18	0.025–12	0.1–4	0.010–1.12	
	°C (h)	(m^2/g)	(m^2/g)	$\log K_{ow}$	5.18	4.76	3.13	2.45	0.46	1.87	2.45	2.20	4.15	4.57	
swine solid	H-250 (4)	1.9	22.4	$\log K_{OC}$ * (mL/g)	6.19	5.36	4.78	4.31	2.97	-	-	-	-	-	[72]
swine solid	P-250 (4)	1.2	29.1	-	5.56	4.31	3.19	2.34	1.55	-	-	-	-	-	[72]
swine solid	P-450 (4)	14.3	139	-	5.85	4.72	3.63	2.91	1.85	-	-	-	-	-	[72]
swine solid	P-600 (4)	5.5	205.6	-	5.71	4.85	4.24	3.07	2.12	-	-	-	-	-	[72]
swine solid	H-250 (20)	4.03	27.2	-	-	-	-	-	-	3.72	3.2	3.42	4.36	5.12	[79]
poultry litter	H-250 (4)	2.8	24.2	-	6.08	5.26	4.53	4.19	2.79	-	-	-	-	-	[72]
poultry litter	P-250 (4)	3	35.1	-	5.33	4.55	3.45	2.68	1.67	-	-	-	-	-	[72]
poultry litter	P-450 (4)	4.8	135.7	-	5.7	4.75	3.76	2.85	1.79	-	-	-	-	-	[72]
poultry litter	P-600 (4)	4.2	150	-	5.78	4.9	4.15	3.21	2.17	-	-	-	-	-	[72]
poultry litter	H-250 (20)	8.77	61.4	-	-	-	-	-	-	3.92	3.49	3.39	4.65	5.41	[79]
poultry litter	P-400 (2–7)	6.71	110.2	-	-	-	-	-	-	3.46	3.2	3.08	3.71	5.48	[79]
wheat straw	P-400 (2–7)	2.08	229.8	-	-	-	-	-	-	3.33	2.78	2.29	3.66	4.96	[79]

* $C_e = 0.005 S_w$; ** $C_e = 0.01 S_w$; C_o—range of initial concentrations of sorbate in solution; C_e—equilibrium concentration, S_w—solubility of compound in water; n.r.—not reported.

In their study of five organic micropollutants on modified HCs from sewage sludge, Kirschhofer et al. [77] did not measure sorption isotherms, but rather % removal of a mixture with low initial concentrations (10–50 µg/L). They compared HCs that were modified by KOH and/or P-removal (N_2-SA: 109–400 m^2/g) to two commercial ACs (N_2-SA: 992–1173 m^2/g) in artificial water and real wastewater samples. The KOH-activated HC was able to remove more than 50% of sulfamethoxazole, diclofenac, and bezafibrate from the artificial water, while the elimination of carbamazepine to nearly 70% and atrazine more than 80% was achieved. Although sorption was reduced in the presence of real wastewater with organic content, the P-reduced activated HC was still able to remove most of the compounds to nearly 45%.

Comparison of five types of thermally and chemically activated HCs from orange peels for their ability to sorb three organic pharmaceuticals showed that thermal activation resulted in sorbents with the highest sorption capacities [82]. They also exhibited the highest surface areas (499–618 m^2/g). Their sorption ability was found to be largely dependent on whether the molecules were ionized and on the porosity developed by the activation step.

3.2.2. Surface and Bulk Properties of HCs

Due to advances in analytical methods, much progress has been made in connecting the effect of the char physicochemical properties with sorption capacity characteristics [90,91]. The relevant system properties can be identified and related to the different sorption mechanisms. Some of the key factors affecting adsorption are: (1) the adsorption process conditions (pH, temperature, contact time, presence of competing compounds) (2) adsorbate (size, charge, and in the case of organic compounds, hydrophobicity, and the presence of specific functional groups); (3) adsorbent (surface area, hydrophobicity, polarity, aromaticity and the presence of H-bond donor/acceptor groups).

The char surface properties are mainly influenced by the feedstock and production method (e.g., pyrolysis, hydrothermal carbonization, vapor-thermal carbonization) [65,84]. Post-processing steps (e.g., washing with water or acetone, activation) can also influence sorbent properties, such as pore volume [5,84] and surface aliphatics [72].

Chars usually display a high degree of aromaticity with a number of oxygen-containing groups on the surface [84,85]. ^{13}C-NMR analysis of HC from glucose revealed that 60% of the carbon atoms are cross-linked furan-based structures directly via either sp^2 or sp^3 type carbon groups [92], in contrast to the higher degree of arene-like structures found in pyrolysis chars from the same substrate [93]. Further ^{13}C-NMR analyses of chars from livestock waste have shown that, while HCs have a larger degree of aromaticity than pyrochars made at the same temperature (~43–55% vs. 26–32%; 250 °C), the aromaticity of pyrochars increases with increasing production temperature, reaching over 90% (600 °C) [72]. The surface groups identified via FTIR and XPS include hydroxyl (–OH), ketone (–CO), ester (–COO–), aldehyde (–CHO), amino ($–NH_2$), nitro ($–NO_2$), phenolic (C_6H_5OH), and carboxyl groups (–COOH) [90]. The bonding of these oxygen-containing polar functional groups of HC via hydrogen bonding to organic sorbates is a common mechanism for many organic compounds, including dyes, phenolics, pesticides, PAHs, and antibiotics [67,68,70].

For inorganics, including cations and anions, sorption due to complexation reactions (with carboxyl and hydroxyl groups) and electrostatic interactions on HCs has often been determined [69,80]. The slightly acidic pH and moderately negatively charged surfaces (zeta potential) of HCs enable them to adsorb sorbates with opposite charges (e.g., methylene blue, lead [84]). The surface hydroxyl, carboxylate, and carbonyl groups showed a high cation exchange capacity, which resulted in the sorption of positively charged sorbates [84]. None of the nine HCs they studied, however, showed significant affinity for the negatively charged phosphate. However, the surface charge of HC, as well as the degree of ionization and the speciation of metal ions can all be influenced by solution pH [93]. This illustrates that many factors affect the sorption process, and further investigations are required to gain understanding to optimize the sorption process.

3.2.3. Adsorption Applications

In order to design continuous sorption systems packed with HC particles, the knowledge of more than the sorption isotherm for single compounds is required. In addition, some other features influencing the process have to be considered, such as char densities and void fractions (bed pressure drop), effect of water matrix on sorption of target sorbates, dynamic sorption and kinetic information of continuous flow fixed-bed adsorbers, or the presence of other compounds on the system and therefore potential competitive adsorption.

Contrary to sorption isotherm experiments studied under batch equilibrium conditions, dynamic experiments, such as sorption column experiments, provide more realistic sorption capacity information for continuous flow adsorbers. The bed depth service time model can be used to estimate the adsorption capacity of the HC adsorbents [13]. Mathematical models describing transport and sorption kinetics of adsorbents can be used to examine the effects of various process variables, such as flow, bed depth, etc. Xue et al. [75] successfully modeled the transport and the sorption kinetics of heavy metals in a column packed with hydrogen peroxide treated HC particles using the advection-dispersion equation coupled with a modified Elovich equation.

An additional factor to be considered in practical applications is the effect of competing compounds on the sorption of target sorbates. In their investigation of the effects of the presence of multiple metals on the sorption capacities of three plant-based HCs (wheat straw/saw dust/corn stalk), Sun et al. [69] evaluated removing Pb, Cd, Cu, and Zn simultaneously. In the presence of all four metals, Cd sorption capacity decreased to 10–15% of that for Cd alone (Table 3). Although the KOH-activated HCs showed 2–3 higher q_c values than untreated ones, both showed a similar reduction in the presence of multiple metals, indicating that there is competition between the metals for surface adsorption sites. They found that the maximum sorption capacity q_c generally followed a trend of Pb (II) > Cu (II) > Cd (II) > Zn (II) for all of the HCs investigated, which coincided with the reverse order of hydrated ionic radius. They postulated that competition from Pb (II) might reduce the sorption of other heavy metals even in the activated HCs, with the increased binding sites associated with oxygen-containing functional groups, such as hydroxyl and carboxyl groups. Xue et al. [90] found a similar order in sorption capacities in their comparison of single and multi-metal sorption studies on H_2O_2 modified-HCs from peanut hulls. The heavy metal removal ability of the modified HC followed the sequence Pb (II) > Cu (II) > Cd (II) > Ni (II). However, they compared the change in sorption capacity for Pb due to the addition of Cu (II), Cd (II), and Ni (II). Lead sorption only decreased by 28%, in contrast to the almost 90% reduction that was found for Cd by Sun et al. [69].

In wastewater and soil applications, minerals and organic matter in the matrix can influence the sorption capacities of the chars. Kirschhofer et al. [77] found that sorption of five organic micropollutants on modified HCs in the presence of real wastewater with high organic content (11.1 g/m^3) was reduced, but that the P-reduced activated HC was still able to remove most of the compounds to nearly 45%. In sorption studies to test the mobility of the herbicide isoproturon in an agricultural soil enriched with either one of three pyro- or HCs, pyrochar reduced the amount of herbicide by a factor of 10–2283, whereas HC only reduced it by a factor of 3–13. While the high sorption values for pyrochars may be good for preventing transport of the herbicide from the field, its target purpose, that of weed reduction, could be jeopardized. Instead, the authors suggest that the soil application of HCs may be an effective management practice to ensure the availability of the herbicide, together with reducing the risk of contamination of water bodies.

3.3. Energy Storage Applications

The use of carbon materials in energy storage applications, such as electrode materials for electrochemical capacitors (ECs) or supercapacitors (EDLCs), has been widely reported. These devices can be used in many portable electronic devices as well as in electric vehicles or cold-starting assistants, and show better performance than secondary batteries due to improved features, such as rate capability and longer cyclic life [94]. Many types of carbon materials have been investigated so,

far such as carbon nanotubes, activated carbons, composite materials, however, the economics and environmental weight associated to some of these processes motivates the search on new and more sustainable synthesis approaches [95]. The previously mentioned advantages of HTC in relation to other thermochemical processes have motivated the investigation of this process to produce energy storage devices from biomass.

The lack in intrinsic porosity associated to biomass-based HTC materials is a decisive handicap for their use in energy storage devices, for which a high surface area and adequate pore size distribution offering short ion-diffusion pathways (mainly microporous but also with presence of large pores) is needed to ensure the efficient transport and diffusion of ions throughout the material. For this reason, only HTC is not enough to yield suitable potential electrode materials and this involves a serious downside, which requires further treatment (or the addition of chemicals to the water solution) to improve porosity development; in this line, different methods have been proposed, as it is described below, which can, to a different extent, downgrade the green character of the whole process.

On the other hand, materials obtained from HTC usually present a favorable, homogeneous distribution of oxygen and nitrogen functionalities on the HC, which can be very interesting for enhancing pseudocapacitance via additional Faradaic reactions and intrinsic catalytic activity in electrochemical devices. For this reason, high protein (and thus, N) and low carbohydrate content precursors are more interesting. Moreover, additional functionalities can be provided into the carbon framework by adding chemicals prior, during, or after HTC treatments. Another interesting point of HCs in relation to their use as supercapacitors is that in this application a high mineral content can improve their behavior and HTC processes can be driven to maximize this feature [67].

Finally, it is worth mentioning that the literature offers a wide variety of works using pure biomass materials (monosaccharides, polysaccharides, aminoacids, proteins, sugars), while heterogeneous biomass has been studied only to a limited extent. Moreover, to the best of the authors' knowledge, HTC alone has not been suitable to produce materials with superconductive properties. However, many authors have successfully implemented two-step processes integrating HTC and chemical activation, obtaining carbon materials with tunable porous structure; furthermore, adding doping substances can help the incorporation of particular functionalities, which enhance the electrode performance. In this field, HTC is therefore regarded as a suitable pretreatment (before pyrolysis), instead of as a process in itself; it can significantly improve the final surface characteristics of the carbons obtained, as compared to classical chemical activation processes [96]. Previous pieces of research have demonstrated that HTC prevents the release of heteroatoms even after high-temperature pyrolysis because they are covalently incorporated into the carbon structure [95]. These heteroatoms are then kept on the carbon after pyrolysis and modify their configuration from sp^3 C–X (X: e.g., C, O, H) into aromatic sp^2 C=C bonds, giving rise to a more dense graphitic structure [97].

A review of the research in this field shows that KOH is, by far, the most used activating agent for enhancing porosity development in HCs in order to improve their supercapacitor performance [98–102], providing a better porosity develpment as compared to other chemical agents such as H_3PO_4 or NaOH [103]. This compound can successfully develop the HC incipient porosity by means of the Reaction (1), followed by K_2CO_3 decomposition into K_2O or its reaction with carbon. Depending on the feedstock and the reaction conditions (of both HTC and activation process), structural properties can be improved.

$$6KOH + 2C \leftrightarrow 2K + 3H_2 + 2K_2CO_3 \quad (12)$$

For example, Ferrero et al. [99] subjected defatted soybean (by-product from soybean oil extraction) to a two-stage process, as follows: the precursor was first hydrocarbonized (200 °C) and then the solid residue was chemically activated using KOH; then, sample annealing was conducted at temperatures in the range 600–800 °C. These authors obtained large surface area materials with a very microporous nature, with a clear improved porosity for higher temperatures (values of S_{BET} up to 2130 $m^2 \cdot g^{-1}$). The activated HCs preserved moderate amounts of N (up to 4%), lower for higher thermal treatment temperature; the surface N was mainly in the form of pyridinic, pirrolic, quaternaty N (N–Q),

and pyridine N–oxides (N–O), whose contribution was also dependent on the activation temperature. Although all of the materials showed a quite good performance, the one that was prepared at greatest temperature showed the best electronic conductivity. These results suggested that the enhanced ion adsorption due to pore availability was the determinant factor, despite the decrease of the contribution of pseudocapacitance to electrode material associated with the lower amount of O and N. These authors also highlighted that although samples obtained at higher temperature had a lower proportion of N, the forms at which this is found in the carbon surface had an impact on the conductive properties, and, in this frame, their greater relative proportion of N–Q and N–O, as well as improved carbon ordering, was beneficial to the electron transfer through the carbon.

Manyala et al. [98] investigated the use of pine cone HCs. The HCs were prepared following an acetone and distilled water washing, then H_2SO_4 assisted HTC at 160 °C, and finally KOH chemical activation (600–900 °C). The resulting materials showed high porosity development (with a mainly mesoporous structure), and 800 °C was chosen as the most interesting temperature, since a further increase gave rise to the collapse of the carbon porous structure. Moreover, long-term stability analyses on the electrodes showed that a slight decay in capacitance was observed only after 60 h, at 1 V.

Jain at al. [101] studied the HTC of coconut shell in the presence of $ZnCl_2$ and H_2O_2 and found that both temperature and $ZnCl_2$ concentration influenced the amount of oxygen groups formed on the HC; this, in turn, facilitated Zn^{2+} access to the precursor surface, which led to better dehydration of the biomass and in definitive enhanced mesopore formation by subsequent chemical activation. Greater concentrations were beneficial for solid yield and oxygen functional group formation, up to a maximum, which was associated with limited solubility at higher concentrations.

Tan et al. [102] investigated the preparation of conductive carbon materials from blends of citric acid and urea, using microwave assisted HTC (MW), followed by pyrolyisis (700 °C) and KOH activation (heating stage at 700–900 °C). This methodology was beneficial for the formation of pyrrolic-N in the graphene framework. Moreover, it was found that increasing activation temperature decreased the N-content and also influenced N-bonding configuration. A similar procedure was followed by Wei et al. [96], who prepared HCs from stem bark from broussonetia papyrifera (HTC at 120 °C in a 1 M KOH solution and subsequent pyrolysis at 600–800 °C). Furthermore, they replicated the process without HTC (that is to say, stem bark was refluxed in a 1 M KOH solution at room temperature prior to pyrolysis), and they found that the obtained carbon had poorer textural and electrochemical performance. In their study, Wei et al. found that the optimal pyrolysis temperature was 800 °C, which gave the highest porosity development (S_{BET} of 1538 $m^2 \cdot g^{-1}$), while the carbon obtained at 700 °C (1212 $m^2 \cdot g^{-1}$) resulted in the best conductive behavior, probably owing to its more favorable pore size distribution (narrower mean porosity) and more appropriate surface chemistry, with greater amount of heteroatoms.

As previously indicated, the literature review gives evidence that KOH chemical activation has so far been the preferred synthesis method to develop porosity in HTC based supercapacitor manufacture. Despite its effectiveness, this chemical also leads to environmental concern due to its corrosive and harmful characteristics because of its strong alkalinity [103]. Therefore, finding effective sustainable synthesis schemes yielding highly porous materials is a challenging issue at the moment. With this in view, Sevilla et al. [104] have recently investigated the production of electrode material from a glucose-derived HC using potassium bicarbonate ($KHCO_3$) as chemical activating agent. They achieved carbon materials with S_{BET} values up to 2230 $m^2 \cdot g^{-1}$. Besides the economic and environmental advantages of using $KHCO_3$ instead of KOH, the authors found a significant increase in yield values and improved surface morphologies because of the greater melting point of the former chemical. The authors postulated that as a result of enhanced CO_2 gasification during thermal treatment at 850 °C, owing to K_2CO_3 decomposition, porosity was increased if long treatment times (5 h) were used. Mesoporosity development was also enhanced by adding melamine to the HTC process, in whose case S_{BET} values up to 3000 $m^2 \cdot g^{-1}$ were achieved; furthermore, while this chemical was also beneficial for providing N-functionalities on the HCs, care must be taken since hydrogen cyanide can be produced during the reaction.

This section cannot be concluded without making a comment on the recent use of biomass derived HCs for microbiological bioelectrochemical applications. Brun et al. [105] investigated the production of enzyme-based biofuel cells from saccharide derivatives (furfural) and phenolic compounds (phloroglucinol), both compounds being isolated from biomass (although they used the pure compounds in their study). Because enzyme loading, responsible for the catalytic activity of these devices, has to be facilitated in these devices, but their desorption has to be avoided during operation, very specific porous structures, with high microporosity, but also large macropore volumes, are needed for this application. These authors hydrocarbonized the above mentioned precursors via a soft emulsion templating methodology followed by pyrolysis and obtained macroporous materials with S_{BET} and total pore volume values of 730 $m^2 \cdot g^{-1}$ and 18 $cm^3 \cdot g^{-1}$, respectively, and a high connectivity within the porous network. These materials, called monolite carbo-HIPEs (HIPE for High Internal Phase Emulsion), were used as support for the inmobilization of glucose oxidase-based biocatalytic mixtures. Despite various chemicals (phloroglucinol, iron chloride hexahydrate, dodecane, polyoxiethylene-20 sorbitan monooleate), the possibility of using biomass derivatives for such an application was outstanding, achieving promising performances towards the oxidation of glucose to gluconolactone. More recently, using 5-HMF and phloroglucinol from fruit tree bark, Flexer et al. [106] manufactured monolitic carbonaceous material (HIPE) by means of chemical HTC followed by pyrolyisis at 740 °C. The HIPE, with a S_{BET} value of 1130 $m^2 \cdot g^{-1}$ and high macropore volume (9 $mL \cdot g^{-1}$), was then used tested as anode material inside a microbial bioelectronical system, aimed to oxidize waste water and produce electricity. The results showed that the so prepared HIPEs had a high biocompatibility and allowed for the long-term activity of the microbial communities within the scaffolds.

3.4. Catalyst

The need for finding more environmentally sustainable routes to synthesize materials or degrade harmful products has also motivated the scientific community towards the search for green catalysts, and, in this field, many different alternatives based on HTC of biomass materials or their derivatives have been reported very recently. Owing to their high stability and tunable surface properties, these materials used themselves or as catalyst supports has proven to be effective in many processes.

In the field of hydrogen production, a large number of studies using HC as a catalyst have been reported. For example, Safari et al. [107] studied the hydrothermal gasification (HTG) of macroalgae with the aim of producing a H_2 rich gas. They found that the HC obtained from these processes had a high ash content and potential catalytic activity, so that they performed similar HTG experiments loading the obtained HCs into the reactor. The catalyst not only promoted H_2 production, but also enhanced phenol formation in the aqueous phase, while acid production was inhibited. Shang et al. [108] investigated the catalytic production of H_2 from room temperature hydrolysis of ammonia borane. Their catalyst, made from sodium polyacrylate assisted HTC (180 °C, 8 h) of glucose, was further pyrolyzed (800 °C, 1 h) and enriched with Ni_x-Pd_y particles. This procedure allowed for them to obtain carbon nanospheres with a uniform distribution of carbon nanoparticles and a value of S_{BET} of 1186 $m^2 \cdot g^{-1}$. Using the catalysts effectively improved the hydrogen production, which was associated to the synergetic interaction between the support and metal nanoparticles. In particular, a turnover frequency of 182 mol H_2 mol $catalyst^{-1}$ min^{-1} at room temperature was obtained; this value was much higher than that obtained using the same procedure, but with a commercial active carbon instead of the HC, and also higher than that found for more expensive metal-precious catalysts.

Biomass HCs have also been used to enhance the degradation of organic compounds and some promising results have been obtained so far. For instance, Gai et al. [109] prepared pine sawdust HC microspheres adding Fe salts to the liquid solution (200 °C, 1 h) and applied them for enhancing phenol degradation (used as tar model compound). Their materials showed a tight Fe embedment and uniform dispersion in the carbon matrix; in addition, the authors demonstrated that both the particle size and porous development of the so obtained HCs could be tuned up. The materials were applied

as catalysts during phenol degradation, providing large catalytic activity, furthermore, these materials showed resistance to coke deposition. Prasannan and Imae [110] synthetisized carbon dots (C-dots) from orange peel HTC and used them as an effective catalyst for the degradation of Naphtol blue-black (NBB) azo dye under UV light irradiation. Their HC synthesis process included previous washing with H_2SO_4 and mixing with hypochlorite previous to HTCF (190 °C, 12 h), and subsequent rinsing with dichloromethane. Afterwards, ZnO diluted in 2-propanol was added to the HC. The resulting material, with spherical morphology, showed a homogeneous dispersion of the metal and resulted to be an effective catalyst for NBB photodegradation, significantly enhancing the removal as compared to the ZnO alone. This improvement was associated to the promotion of the transmission of the photogenerated species by providing additional flowing pathways via electron accepting and electron transporting C-dots, owing to the presence of oxygen surface groups.

Finally, due to their rich and tunable surface functionalities (mainly oxygen ones), biomass HCs have been used in many carbo-catalyzed reactions in which specific active sites are needed, providing a more simple and environmental benign route, without the addition of acids, such as HNO_3 or H_2SO_4, to create such functionalities. Some examples are nitrobenzene reduction and Beckmann rearrangement reactions, using glucose HC [111] and glyceron etherification [112].

4. Conclusions

Past years have witnessed the effectiveness of hydrothermal carbonization as a purposeful and cost-effective methodology to convert biomass or other solid wastes to added-value products. This work reviewed the recent research made on the study of the process itself and on the final applications of the solid phase (excluding soil amendment), and allowed for to obtain the following conclusions:

- The influence of experimental variables (temperature, time, and biomass type and loading) on hydrothermal carbonization has been studied extensively. In general, the most commonly reported HC property is HC yield and the second most reported property is HC carbon content. Generally, reaction temperature has the greatest influence on the process, while the others can have a lower or greater relevance in the process depending on the particular reaction conditions; a great interdependence between variables exists. As temperature increases, solid yields and HC oxygen contents decrease and HC carbon content increases, with an enhancement of the heating value. This variable has also been shown to influence carbonization rates, with higher temperatures being correlated with the accelerating of carbonization reactions.
  Reaction time, less studied, is also important, primarily at early times and its influence on carbonization product characteristics is also likely dependent on reactor heating time and/or heating rate, although the wide range of experimental conditions shown in the bibliography and the participation of complex reactions whose relevance changes with time hinders the comprehension of the process.
- Statistic (linear and non-linear models), kinetic models (assuming first-order relationships), shrinking core, and severity factor-based relationships have been developed to predict HC properties. Universal application of the majority of these models may be limited because they are based on data from individual studies. The development of a model, including temperature as a function of time, while considering heat transfer mechanisms, is very promising since it might allow the study of any installation.
- Biomass hydrochars have the potential to be used as adsorbent for wastewater treatment. Despite their scant porosity, the tunable surface chemistry can enhance adsorption selectivity and some promising results have been obtained for organic compounds, heavy metals, and emerging contaminants. Moreover, the joint of chemical and physical activation can improve their performance as a result of pore development. In general, equilibrium adsorption data fit well Langmuir and Freundlich models, and values of adsorption capacity of the same order of magnitude than those obtained using commercial activated carbons are obtained.

- The use of biomass hydrochars as fuels in combustion and gasification processes has also been studied. In this frame, most of the studies have been performed by thermogravimetry, and little literature is found on real installations. Even so, it has been assessed that hydrothermal carbonization as pretreatment can improve the production of syngas and also some important combustion (and co-combustion) features, such as activation energy, ash related issues, and harmful emissions. Moreover, demonstrated improved pelletization as a result of hydrothermal carbonization is very important for this application.
- Finally, some works on the use of biomass hydrochars as low cost catalysts and as suitable as electrode material in energy storage applications, such as supercondensers, have been reported. In general, HTC alone was not enough to develop competitive materials and additional processes (pyrolysis, chemical activation, blending...) were needed prior, during, or after the process to alter the surface functionality or the structure of the hydrochars. While the incorporation of these steps involved the use of chemicals or energy, and therefore downgrades the green character of the whole process, the method still provides important advantages, such as the use of waste, which is already a highlighting and inspiring advantage. However, more research aimed to further include more sustainable production pathways in this field should be addressed.

Supplementary Materials: The following are available online at www.mdpi.com/1996-1073/10/1/216/s1, Figure S1: SY level curves [25], Table S1: Percentage of Collected Papers that Report Specific Hydrochar Properties, Table S2: Influence of changing feedstocks in relevant collected carbonization studies, Table S3: Influence of process related parameters in relevant collected carbonization studies, Table S4: Influence of changing feedstocks in relevant collected carbonization studies.

Acknowledgments: This work has received funding from "Junta de Extremadura" through project GR15034, and from "Ministerio de Economía y Competitividad", via projects CTM2014-55998-R and CTM2016-75937-R. This research was supported by the USDA-ARS National Program 212. Mention of trade names or commercial products is solely for the purpose of providing specific information and does not imply recommendation or endorsement by the U.S. Department of Agriculture. NDB acknowledges the support of the National Science Foundation under Grant No. 1055327. The authors have received funds for covering the costs to publish in open access.

Author Contributions: This review was conceived by mutual agreement of all the authors; all of them shared the work and then reviewed each section. S.R. wrote the introduction and energy storage section, J.L., K.R. and S.B. worked thoughtfully on the section devoted to adsorption applications, N.B. and L.L. wrote the section on the studies and models on HC properties predictions (Section 2.2), E.S. wrote Section 2.1 (Kinetics mathematical modeling), and A.Á. and B.L. worked on Section 3.1 (application as biofuel) and 3.4 (as catalyst), respectively.

Conflicts of Interest: The authors declare no conflict of interest.

References

1. Fang, J.; Zhan, L.; Ok, Y.S.; Gao, B. Minireview of potential applications of hydrochar derived from hydrothermal carbonization of biomass. *J. Ind. Eng. Chem.* **2018**, *57*, 15–21. [CrossRef]
2. Berge, N.D.; Ro, K.S.; Mao, J.; Flora, J.R.V. Hydrothermal Carbonization of Municipal Waste Streams. *Environ. Sci. Technol.* **2011**, *45*, 5696–5703. [CrossRef] [PubMed]
3. Lin, Y.; Ma, X.; Peng, X.; Hu, S.; Yu, Z.; Fang, S. Effect of hydrothermal carbonization temperature on combustion behavior of HC fuel from paper sludge. *Appl. Therm. Eng.* **2015**, *91*, 574–582. [CrossRef]
4. Román, S.; Nabais, J.M.V.; Laginhas, C.; Ledesma, B.; González, J.F. Hydrothermal carbonization as an effective way of densifying the energy content of biomass. *Fuel Process. Technol.* **2012**, *103*, 78–83. [CrossRef]
5. Román, S.; Nabais, J.M.V.; Ledesma, B.; González, J.F.; Laginhas, C.; Titirici, M.M. Production of low-cost adsorbents with tunable surface chemistry by conjunction of hydrothermal carbonization and activation processes. *Microporous Mesoporous Mater.* **2013**, *165*, 127–133. [CrossRef]
6. Reza, M.T.; Uddin, M.H.; Lynam, J.G.; Coronella, C.J. Engineered pellets from dry torrefied and HTC biochar blends. *Biomass Bioenergy* **2014**, *63*, 229–238. [CrossRef]
7. Danso-Boateng, E.; Holdich, R.G.; Shama, G.; Wheatley, A.D.; Sohail, M.; Martin, S.J. Kinetics of faecal biomass hydrothermal carbonisation for HC production. *Appl. Energy* **2013**, *111*, 351–357. [CrossRef]
8. Braghiroli, F.L.; Fierro, V.; Izquierdo, M.T.; Parmentier, J.; Pizzi, A.; Celzard, A. Kinetics of the hydrothermal treatment of tannin for producing carbonaceous microspheres. *Bioresour. Technol.* **2015**, *151*, 271–277. [CrossRef] [PubMed]

9. Knežević, D.; van Swaaij, W.; Kersten, S. Hydrothermal Conversion of Biomass. I. Glucose Conversion in Hot Compressed Water. *Ind. Eng. Chem. Res.* **2009**, *48*, 4731–4743. [CrossRef]
10. Reza, M.T.; Yan, W.; Uddin, M.H.; Lynam, J.G.; Hoekman, S.K.; Coronella, C.J.; Vásquez, V.R. Reaction kinetics of hydrothermal carbonization of loblolly pine. *Bioresour. Technol.* **2013**, *139*, 161–169. [CrossRef] [PubMed]
11. Iryani, D.A.; Kumagai, S.; Nonaka, M.; Sasaki, K.; Hirajima, T. Hydrothermal carbonization kinetics of sugarcane bagasse treated by hot compressed water under variable temperature conditions. *ARPN J. Eng. Appl. Sci.* **2016**, *11*, 4833–4839.
12. Jatzwauck, M.; Schumpe, A. Kinetics of hydrothermal carbonization (HTC) of soft rush. *Biomass Bioenergy* **2015**, *75*, 94–100. [CrossRef]
13. Ro, K.; Lima, I.; Reddy, G.; Jackson, M.; Gao, B. Removing Gaseous NH_3 Using Biochar as an Adsorbent. *Agriculture* **2015**, *5*, 991–1002. [CrossRef]
14. Jung, D.; Kruse, A. Evaluation of Arrhenius-type overall kinetic equations for hydrothermal carbonization. *J. Anal. Appl. Pyrolysis* **2017**, *127*, 286–291. [CrossRef]
15. Ruyter, H.P. Coalification model. *Fuel* **1982**, *61*, 1182–1187. [CrossRef]
16. Abatzoglou, N.; Chornet, E.; Belkacemi, K.; Overend, R.P. Phenomenological kinetics of complex systems: The development of a generalized severity parameter and its application to lignocellulosics fractionation. *Chem. Eng. Sci.* **1992**, *47*, 1109–1122. [CrossRef]
17. Gao, Y.; Yu, B.; Wu, K.; Yuan, Q.X.; Wang, X.H.; Chen, H.P. Physicochemical, pyrolytic, and combustion characteristics of HC obtained by hydrothermal carbonization of biomass. *Bioresources* **2016**, *11*, 4113–4133. [CrossRef]
18. Hoekman, S.K.; Broch, A.; Felix, L.; Farthing, W. Hydrothermal carbonization (HTC) of loblolly pine using a continuous, reactive twin-screw extruder. *Energy Convers. Manag.* **2017**, *134*, 247–259. [CrossRef]
19. Janga, K.K.; Øyaas, K.; Hertzberg, T.; Moe, S.T. Application of a pseudo-kinetic generalized severity model to the concentrated sulfuric acid hydrolysis of pinewood and aspenwood. *BioResources* **2012**, *7*, 2728–2741.
20. Suwelack, K.U.; Wüst, D.; Fleischmann, P.; Kruse, A. Prediction of gaseous, liquid and solid mass yields from hydrothermal carbonization of biogas digestate by severity parameter. *Biomass Convers. Biorefinery* **2016**, *6*, 151–160. [CrossRef]
21. Gallifuoco, A.; Taglieri, L.; Scimia, F.; Papa, A.A.; Di Giacomo, G. Hydrothermal carbonization of Biomass: New experimental procedures for improving the industrial Processes. *Bioresour. Technol.* **2017**, *244*, 160–165. [CrossRef] [PubMed]
22. Mäkela, M. Experimental design and response surface methodology in energy applications: A tutorial review. *Energy Convers. Manag.* **2017**, *151*, 630–640. [CrossRef]
23. Heilmann, S.M.; Davis, H.T.; Jader, L.R.; Lefebvre, P.A.; Sadowsky, M.J.; Schendel, F.J.; von Keitz, M.G.; Valentas, K.J. Hydrothermal carbonization of microalgae. *Biomass Bioenergy* **2010**, *34*, 875–882. [CrossRef]
24. Álvarez-Murillo, A.; Román, S.; Ledesma, B.; Sabio, E. Study of variables in energy densification of olive stone by hydrothermal carbonization. *J. Anal. Appl. Pyrolysis* **2015**, *113*, 307–314. [CrossRef]
25. Sabio, E.; Álvarez-Murillo, A.; Román, S.; Ledesma, B. Conversion of tomato-peel waste into solid fuel by hydrothermal carbonization: Influence of the processing variables. *Waste Manag.* **2016**, *47*, 122–132. [CrossRef] [PubMed]
26. Danso-Boateng, E.; Shama, G.; Wheatley, A.D.; Martin, S.J.; Holdich, R.G. Hydrothermal carbonisation of sewage sludge: Effect of process conditions on product characteristics and methane production. *Bioresour. Technol.* **2015**, *177*, 318–327. [CrossRef] [PubMed]
27. Kannan, S.; Gariepy, Y.; Vijaya Raghavan, G.S. Optimization and characterization of hydrochar produced from microwave hydrothermal carbonization of fish waste. *Waste Manag.* **2017**, *65*, 159–168. [CrossRef] [PubMed]
28. Mäkelä, M.; Benavente, V.; Fullana, A. Hydrothermal carbonization of industrial mixed sludge from a pulp and paper mill. *Bioresour. Technol.* **2016**, *200*, 444–450. [CrossRef] [PubMed]
29. Álvarez-Murillo, A.; Sabio, E.; Ledesma, B.; Román, S.; González-García, C.M. Generation of biofuel from hydrothermal carbonization of cellulose. Kinetics modeling. *Energy* **2016**, *94*, 600–608. [CrossRef]
30. Sabzo, N.; Baloch, H.; Griffin, G.J.; Mubarak, N.M.; Bhutto, A.W.; Abrod, R.; Mazari, S.A.; Alie, B.S. An overview of effect of process parameters on hydrothermal carbonization of biomass. *Renew. Sustain. Energy Rev.* **2017**, *73*, 1289–1299.

31. Falco, C.; Baccile, N.; Titirici, M.-M. Green Chemistry Morphological and structural differences between glucose, cellulose and lignocellulosic biomass derived hydrothermal carbons. *Green Chem.* **2011**, *13*, 3273–3281. [CrossRef]
32. Hoekman, S.K.; Broch, A.; Robbins, C. Hydrothermal Carbonization (HTC) of Lignocellulosic Biomass. *Energy Fuels* **2011**, *25*, 1802–1810. [CrossRef]
33. Hwang, I.-H.; Aoyama, H.; Matsuto, T.; Nakagishi, T.; Matsuo, T. Recovery of solid fuel from municipal solid waste by hydrothermal treatment using subcritical water. *Waste Manag.* **2012**, *32*, 410–416. [CrossRef] [PubMed]
34. Kieseler, S.; Neubauer, Y.; Zobel, N. Ultimate and Proximate Correlations for Estimating the Higher Heating Value of Hydrothermal Solids. *Energy Fuels* **2013**, *27*, 908–918. [CrossRef]
35. Liu, Z.; Quek, A.; Kent Hoekman, S.; Balasubramanian, R. Production of solid biochar fuel from waste biomass by hydrothermal carbonization. *Fuel* **2013**, *103*, 943–949. [CrossRef]
36. Lu, X.; Pellechia, P.J.; Flora, J.R.V.; Berge, N.D. Influence of reaction time and temperature on product formation and characteristics associated with the hydrothermal carbonization of cellulose. *Bioresour. Technol.* **2013**, *138*, 180–190. [CrossRef] [PubMed]
37. Luo, G.; Shi, W.; Chen, X.; Ni, W.; Strong, P.J.; Jia, Y.; Wang, H. Hydrothermal conversion of water lettuce biomass at 473 or 523 K. *Biomass Bioenergy* **2011**, *35*, 4855–4861. [CrossRef]
38. Akalın, M.K.; Tekin, K.; Karagoz, S. Hydrothermal liquefaction of cornelian cherry stones for bio-oil production. *Bioresour. Technol.* **2012**, *110*, 682–687. [CrossRef] [PubMed]
39. Jamari, S.S.; Howse, J.R. The effect of the hydrothermal carbonization process on palm oil empty fruit bunch. *Biomass Bioenergy* **2012**, *47*, 82–90. [CrossRef]
40. Li, L.; Diederick, R.; Flora, J.R.V.; Berge, N.D. Hydrothermal carbonization of food waste and associated packaging materials for energy source generation. *Waste Manag.* **2013**, *33*, 2478–2492. [CrossRef] [PubMed]
41. Lu, X.; Jordan, B.; Berge, N.D. Thermal conversion of municipal solid waste via hydrothermal carbonization: Comparison of carbonization products to products from current waste management techniques. *Waste Manag.* **2012**, *32*, 1353–1365. [CrossRef] [PubMed]
42. Cao, X.; Ro, K.S.; Libra, C.I.; Kammann, C.I.; Lima, I.; Libra, J.; Li, L.; Li, Y.; Chen, N.; Yang, J. Effects of biomass types and carbonization conditions on the chemical characteristics of hydrochars. *J. Agric. Food Chem.* **2013**, *61*, 9401–9411. [CrossRef] [PubMed]
43. Garcia Alba, L.; Torri, C.; Samori, C.; van der Spek, J.; Fabbri, D.; Kersten, S.R.A.; Brilman, D.W.F. Hydrothermal Treatment (HTT) of Microalgae: Evaluation of the Process as Conversion Method in an Algae Biorefinery Concept. *Energy Fuels* **2012**, *26*, 642–657. [CrossRef]
44. Kang, S.; Li, X.; Fan, J.; Chang, J. Solid fuel production by hydrothermal carbonization of black liquor. *Bioresour. Technol.* **2012**, *110*, 715–718. [CrossRef] [PubMed]
45. Gao, Y.; Wang, X.H.; Yang, H.P.; Chen, H.P. Characterization of products from hydrothermal treatments of cellulose. *Energy* **2012**, *42*, 457–465. [CrossRef]
46. Mumme, J.; Eckervogt, L.; Pielert, J.; Diakité, M.; Rupp, F.; Kern, J. Hydrothermal carbonization of anaerobically digested maize silage. *Bioresour. Technol.* **2011**, *102*, 9255–9260. [CrossRef] [PubMed]
47. Lu, X.; Berge, N. Influence of feedstock chemical composition on product formation and characteristics derived from the hydrothermal carbonization of mixed feedstocks. *Bioresour. Technol.* **2014**, *166*, 120–131. [CrossRef] [PubMed]
48. Sevilla, M.; Fuertes, A.B. Sustainable porous carbons with a superior performance for CO_2 capture. *Energy Environ. Sci.* **2011**, *4*, 1765–1771. [CrossRef]
49. Tremel, A.; Stemann, J.; Herrmann, M.; Erlach, B.; Spliethoff, H. Entrained flow gasification of biocoal from hydrothermal carbonization. *Fuel* **2012**, *102*, 396–403. [CrossRef]
50. Wiedner, K.; Naisse, C.; Rumpel, C.; Pozzi, A.; Wieczorek, P.; Glaser, B. Chemical modification of biomass residues during hydrothermal carbonization: What makes the difference, temperature or feedstock? *Org. Geochem.* **2013**, *54*, 91–100. [CrossRef]
51. Xiao, L.-P.; Shi, Z.-J.; Xu, F.; Sun, R.-C. Hydrothermal carbonization of lignocellulosic biomass. *Bioresour. Technol.* **2012**, *118*, 619–623. [CrossRef] [PubMed]
52. Titirici, M.-M.; Antonietti, M.; Baccile, N. Hydrothermal carbon from biomass: A comparison of the local structure from poly- to monosaccharides and pentoses/hexoses. *Green Chem.* **2008**, *10*, 1204–1212. [CrossRef]

53. Dinjus, E.; Kruse, A.; Tröger, N. Hydrothermal Carbonization—1. Influence of Lignin in Lignocelluloses. *Chem. Eng. Technol.* **2011**, *34*, 2037–2043. [CrossRef]
54. Mäkela, M.; Fullana, A.; Yoshikawa, K. Ash behaviour during hydrothermal treatment for solid fuel applications. Part 1: Overview of different feedstock. *Energy Convers. Manag.* **2016**, *121*, 402–408. [CrossRef]
55. Li, L.; Flora, J.R.V.; Caicedo, J.M.; Berge, N.D. Investigating the role of feedstock properties and process conditions on products formed during the hydrothermal carbonization of organics using regression techniques. *Bioresour. Technol.* **2015**, *187*, 263–274. [CrossRef] [PubMed]
56. Kannan, S.; Gariepy, Y.; Raghavan, G.S.V. Optimization and Characterization of Hydrochar Derived from Shrimp Waste. *Energy Fuels* **2017**, *31*, 4068–4077. [CrossRef]
57. Nizamuddin, S.; Mubarak, N.M.; Tiripathi, M.; Jayakumar, N.S.; Sahu, J.N.; Ganesan, P. Chemical, dielectric and structural characterization of optimized hydrochar produced from hydrothermal carbonization of palm shell. *Fuel* **2016**, *163*, 88–97. [CrossRef]
58. Guo, S.; Dong, X.; Wu, T.; Zhu, C. Influence of reaction conditions and feedstock on hydrochar properties. *Energy Convers. Manag.* **2016**, *123*, 95–103. [CrossRef]
59. Titirici, M.M.; White, R.J.; Brun, N.; Budarin, V.L.; Su, D.S.; del Monte, F.; Clark, J.H.; MacLachlan, M.J. Sustainable carbon materials. *Chem. Soc. Rev.* **2015**, *44*, 250–290. [CrossRef] [PubMed]
60. He, C.; Wang, K.; Yang, Y.; Wang, J.-Y. Utilization of Sewage-Sludge-Derived Hydrochars toward Effi cient Co-combustion with Different-Rank Coals: Effects of Subcritical Water Conversion and Blending Scenarios. *Energy Fuels* **2014**, *28*, 6140–6150. [CrossRef]
61. Reza, M.T.; Andert, J.; Wirth, B.; Busch, D.; Pielert, J.; Lynam, J.G.; Mumme, J. Hydrothermal Carbonization of Biomass for Energy and Crop Production. *Appl. Bioenergy* **2014**, *1*, 11–27. [CrossRef]
62. Saari, J.; Sermyagina, E.; Kaikko, J.; Vakkilainen, E.; Sergeev, V. Integration of hydrothermal carbonization and a CHP plant: Part 2—Operational and economic analysis. *Energy* **2016**, *113*, 574–585. [CrossRef]
63. Licursi, D.; Antonetti, C.; Fulignati, S.; Vitolo, S.; Puccini, M.; Ribechini, E.; Bernazzani, L.; Raspolli Galletti, A.M. In-depth characterization of valuable char obtained from hydrothermal conversion of hazelnut shells to levulinic acid. *Bioresour. Technol.* **2017**, *244*, 880–888. [CrossRef] [PubMed]
64. Moon, J.; Mun, T.-Y.; Yang, W.; Lee, U.; Hwang, J.; Jang, E.; Choi, C. Effects of hydrothermal treatment of sewage sludge on pyrolysis and steam gasification. *Energy Convers. Manag.* **2015**, *103*, 401–407. [CrossRef]
65. Lin, Y.; Ma, X.; Peng, X.; Yu, Z.; Fang, S.; Lin, Y.; Fan, Y. Combustion, pyrolysis and char CO_2-gasification characteristics of hydrothermal carbonization solid fuel from municipal solid wastes. *Fuel* **2016**, *181*, 905–915. [CrossRef]
66. Gunarathne, D.S.; Mueller, A.; Fleck, S.; Kolb, T.; Chmielewski, J.K.; Yang, W.; Blasiak, W. Gasification characteristics of hydrothermal carbonized biomass in an updraft pilot-scale gasifier. *Energy Fuels* **2014**, *28*, 1992–2002. [CrossRef]
67. Jain, A.; Balasubramanian, R.; Srinivasan, M.P. Hydrothermal conversion of biomass waste to activated carbon with high porosity: A review. *Chem. Eng. J.* **2016**, *283*, 789–805. [CrossRef]
68. Mohan, D.; Sarswat, A.; Ok, Y.S.; Pittman, C.U., Jr. Organic and inorganic contaminants removal from water with biochar, a renewable, low cost and sustainable adsorbent—A critical review. *Bioresour. Technol.* **2014**, *160*, 191–202. [CrossRef] [PubMed]
69. Sun, K.; Tang, J.; Gong, Y.; Zhang, H. Characterization of potassium hydroxide (KOH) modified hydrochars from different feedstocks for enhanced removal of heavy metals from water. *Environ. Sci. Pollut. Res.* **2015**, *22*, 16640–16651. [CrossRef] [PubMed]
70. Li, Y.; Meas, A.; Shan, S.; Yang, R.; Gai, X. Production and optimization of bamboo hydrochars for adsorption of Congo red and 2-naphthol. *Bioresour. Technol.* **2016**, *207*, 379–386. [CrossRef] [PubMed]
71. Regmi, P.; Garcia Moscoso, J.L.; Kumar, S.; Cao, X.; Mao, J.; Schafran, G. Removal of copper and cadmium from aqueous solution using switchgrass biochar produced via hydrothermal carbonization process. *J. Environ. Manag.* **2012**, *109*, 61–69. [CrossRef] [PubMed]
72. Han, L.; Ro, K.S.; Sun, K.; Sun, H.; Wang, Z.; Libra, J.A.; Xing, B. New Evidence for High Sorption Capacity of Hydrochar for Hydrophobic Organic Pollutants. *Environ. Sci. Technol.* **2016**, *50*, 13274–13282. [CrossRef] [PubMed]
73. Han, L.; Sun, H.; Ro, K.S.; Sun, K.; Libra, J.A.; Xing, B. Removal of antimony (III) and cadmium (II) from aqueous solution using animal manure-derived hydrochars and pyrochars. *Bioresour. Technol.* **2017**, *234*, 77–85. [CrossRef] [PubMed]

74. Pellera, F.M.; Giannis, A.; Kalderis, D.; Anastasiadou, K.; Stegmann, R.; Wang, J.Y.; Gidarakos, E. Adsorption of Cu(II) ions from aqueous solutions on biochars prepared from agricultural by-products. *J. Environ. Manag.* **2012**, *96*, 35–42. [CrossRef] [PubMed]
75. Xue, Y.; Gao, B.; Yao, Y.; Inyang, M.; Zhang, M.; Zimmerman, A.R.; Ro, K.S. Hydrogen peroxide modification enhances the ability of biochar (hydrochar) produced from hydrothermal carbonization of peanut hull to remove aqueous heavy metals: Batch and column tests. *Chem. Eng. J.* **2012**, *200–202*, 673–680. [CrossRef]
76. Zhou, N.; Chen, H.; Xi, J.; Yao, D.; Zhou, Z.; Tian, Y.; Lu, X. Biochars with excellent Pb(II) adsorption property produced from fresh and dehydrated banana peels via hydrothermal carbonization. *Bioresour. Technol.* **2017**, *232*, 204–210. [CrossRef] [PubMed]
77. Kirschhöfer, F.; Sahin, O.; Becker, G.C.; Meffert, F.; Nusser, M.; Anderer, G.; Kusche, S.; Klaeusli, T.; Kruse, A.; Brenner-Weiss, G. Wastewater treatment—Adsorption of organic micropollutants on activated HTC-carbon derived from sewage sludge. *Water Sci. Technol.* **2016**, *73*, 607–616. [CrossRef] [PubMed]
78. Koottatep, T.; Fakkaew, K.; Tajai, N.; Polprasert, C. Isotherm models and kinetics of copper adsorption by using hydrochar produced from hydrothermal carbonization of faecal sludge. *J. Water Sanit. Hyg. Dev.* **2017**. [CrossRef]
79. Sun, K.; Gao, B.; Ro, K.S.; Novak, J.M.; Wang, Z.; Herbert, S.; Xing, B. Assessment of herbicide sorption by biochars and organic matter associated with soil and sediment. *Environ. Pollut.* **2012**, *163*, 167–173. [CrossRef] [PubMed]
80. Eibisch, N.; Schroll, R.; Fuß, R.; Mikutta, R.; Helfrich, M.; Flessa, H. Pyrochars and hydrochars differently alter the sorption of the herbicide isoproturon in an agricultural soil. *Chemosphere* **2015**, *119*, 155–162. [CrossRef] [PubMed]
81. Zhu, X.; Liu, Y.; Zhou, C.; Luo, G.; Zhang, S.; Chen, J. A novel porous carbon derived from hydrothermal carbon for efficient adsorption of tetracycline. *Carbon* **2014**, *77*, 627–636. [CrossRef]
82. Fernandez, M.E.; Ledesma, B.; Román, S.; Bonelli, P.R.; Cukierman, A.L. Development and characterization of activated hydrochars from orange peels as potential adsorbents for emerging organic contaminants. *Bioresour. Technol.* **2015**, *183*, 221–228. [CrossRef] [PubMed]
83. Sun, K.; Ro, K.; Guo, M.; Novak, J.; Mashayekhi, H.; Xing, B. Sorption of bisphenol A, 17α-ethinyl estradiol and phenanthrene on thermally and hydrothermally produced biochars. *Bioresour. Technol.* **2011**, *102*, 5757–5763. [CrossRef] [PubMed]
84. Fang, J.; Gao, B.; Chen, J.; Zimmerman, A.R. Hydrochars derived from plant biomass under various conditions: Characterization and potential applications and impacts. *Chem. Eng. J.* **2015**, *267*, 253–259. [CrossRef]
85. Fang, J.; Gao, B.; Zimmerman, A.R.; Ro, K.S.; Chen, J. Physically (CO_2) activated hydrochars from hickory and peanut hull: Preparation, characterization, and sorption of methylene blue, lead, copper, and cadmium. *RSC Adv.* **2016**, *6*, 24906–24911. [CrossRef]
86. Kim, H.-W.; Bae, S.; Lee, J.-Y. A Study on the Removal of Heavy Metals in Soil by Sewage Sludge Biochar. *J. Soil Groundw. Environ.* **2013**, *18*, 58–64. [CrossRef]
87. Elaigwu, S.E.; Rocher, V.; Kyriakou, G.; Greenway, G.M. Removal of Pb^{2+} and Cd^{2+} from aqueous solution using chars from pyrolysis and microwave-assisted hydrothermal carbonization of *Prosopis africana* shell. *J. Ind. Eng. Chem.* **2014**, *20*, 3467–3473. [CrossRef]
88. Gwenzi, W.; Chaukura, N.; Noubactep, C.; Mukome, F.N.D. Biochar-based water treatment systems as a potential low-cost and sustainable technology for clean water provision. *J. Environ. Manag.* **2017**, *197*, 732–749. [CrossRef] [PubMed]
89. Inyang, M.; Dickenson, E. The potential role of biochar in the removal of organic and microbial contaminants from potable and reuse water: A review. *Chemosphere* **2015**, *134*, 232–240. [CrossRef] [PubMed]
90. Kambo, H.S.; Dutta, A. A comparative review of biochar and hydrochar in terms of production, physico-chemical properties and applications. *Renew. Sustain. Energy Rev.* **2015**, *45*, 359–378. [CrossRef]
91. Nartey, D.; Zhao, B. Biochar Preparation, Characterization, and Adsorptive Capacity and Its Effect on Bioavailability of Contaminants: An Overview. *Adv. Mater. Sci. Eng.* **2014**, *2014*, 715398. [CrossRef]
92. Baccile, N.; Laurent, G.; Babonneau, F.; Fayon, F.; Titirici, M.-M.; Antonietti, M. Structural Characterization of Hydrothermal Carbon Spheres by Advanced Solid-State MAS ^{13}C NMR Investigations. *J. Phys. Chem. C* **2009**, *113*, 9644–9654. [CrossRef]
93. Falco, C.; Perez Caballero, F.; Babonneau, F.; Gervais, C.; Laurent, G.; Titirici, M.-M.; Baccile, N. Hydrothermal Carbon from Biomass: Structural Differences between Hydrothermal and Pyrolyzed Carbons via ^{13}C Solid State NMR. *Langmuir* **2011**, *27*, 14460–14471. [CrossRef] [PubMed]

94. Béguin, F.; Presser, V.; Balducci, A.; Frackowiak, E. Carbons and Electrolytes for Advanced Supercapacitors. *Adv. Mater.* **2014**, *26*, 2219–2251. [CrossRef] [PubMed]
95. Wang, J.; Nie, P.; Ding, B.; Dong, S.; Hao, X.; Dou, H.; Zhang, X. Biomass derived carbon for energy storage devices. *J. Mater. Chem. A* **2017**, *5*, 2411–2428. [CrossRef]
96. Wei, T.; Wei, X.; Gao, Y.; Li, H. Large scale production of biomass-derived nitrogen-doped porous carbon materials for supercapacitors. *Electrochim. Acta* **2015**, *169*, 186–194. [CrossRef]
97. Liu, X.; Giordano, C.; Antonietti, M. A Facile Molten-Salt Route to Graphene Synthesis. *Small* **2014**, *10*, 193–200. [CrossRef] [PubMed]
98. Manyala, N.; Bello, A.; Barzegar, F.; Khaleed, A.A.; Momodu, D.Y.; Dangbegnon, J.K. Coniferous pine biomass: A novel insight into sustainable carbon materials for supercapacitors electrode. *Mater. Chem. Phys.* **2016**, *182*, 139–147. [CrossRef]
99. Ferrero, G.A.; Fuertes, A.B.; Sevilla, M. From Soybean residue to advanced supercapacitors. *Sci. Rep.* **2015**, *5*, 16618. [CrossRef] [PubMed]
100. Ding, L.; Zou, B.; Li, Y.; Wang, Z.; Zhao, C.; Su, Y.; Guo, Y. The production of hydrochar-based hierarchical porous carbons for use as electrochemical supercapacitor electrode materials. *Colloids Surf. A Phys. Eng. Aspects* **2013**, *423*, 104–111. [CrossRef]
101. Jain, A.; Xu, C.; Jayaraman, S.; Balasubramanian, R.; Lee, J.Y.; Srinivasan, M.P. Mesoporous activated carbons with enhanced porosity by optimal hydrothermal pre-treatment of biomass for supercapacitor applications. *Microporous Mesoporous Mater.* **2015**, *218*, 55–61. [CrossRef]
102. Tan, J.; Chen, H.; Gao, Y.; Li, H. Nitrogen-doped porous carbons derived from citric acid and urea with outstanding supercapacitance performance. *Electrochim. Acta* **2015**, *178*, 144–152. [CrossRef]
103. Deng, J.; Li, M.; Wang, Y. Biomass-derived carbon: Synthesis and applications in energy storage and conversion. *Green Chem.* **2016**, *18*, 4824–4854. [CrossRef]
104. Sevilla, M.; Fuertes, A.B. A Green Approach to High-Performance Supercapacitor Electrodes: The Chemical Activation of Hydrochar with Potassium Bicarbonate. *ChemSusChem* **2016**, *9*, 1880–1888. [CrossRef] [PubMed]
105. Brun, N.; Edembe, L.; Gounel, S.; Mano, N.; Titirici, M.M. Emulsion-Templated Macroporous Carbons Synthesized by Hydrothermal Carbonization and Their Application for the Enzymatic Oxidation of Glucose. *ChemSusChem* **2013**, *6*, 701–710. [CrossRef] [PubMed]
106. Flexer, V.; Donose, B.C.; Lefebvre, C.; Pozo, G.; Boone, M.N.; Van Hoorebeke, L.; Baccour, M.; Bonnet, L.; Calas-Etienne, S.; Galarneau, A.; et al. Microcellular Electrode Material for Microbial Bioelectrochemical Systems Synthesized by Hydrothermal Carbonization of Biomass Derived Precursors. *ACS Sustain. Chem. Eng.* **2016**, *4*, 2508–2516. [CrossRef]
107. Safari, F.; Norouzi, O.; Tavasoli, A. Hydrothermal gasification of *Cladophora glomerata macroalgae* over its HC as a catalyst for hydrogen-rich gas production. *Bioresour. Technol.* **2016**, *222*, 232–241. [CrossRef] [PubMed]
108. Shang, N.; Zhou, X.; Feng, C.; Gao, S.; Wu, Q.; Wang, C. Synergetic catalysis of Ni Pd nanoparticles supported on biomass-derived carbon spheres for hydrogen production from ammonia borane at room temperature. *Int. J. Hydrogen Energy* **2017**, *42*, 5733–5740. [CrossRef]
109. Gai, C.; Zhang, F.; Lang, Q.; Liu, T.; Peng, N.; Liu, Z. Facile one-pot synthesis of iron nanoparticles immobilized into theporous hydrochar for catalytic decomposition of phenol. *Appl. Catal. B Environ.* **2017**, *204*, 566–576. [CrossRef]
110. Prasannan, A.; Imae, T. One-Pot Synthesis of Fluorescent Carbon Dots from Orange Waste Peels. *Ind. Eng. Chem. Res.* **2013**, *52*, 15673–15678. [CrossRef]
111. Wen, G.; Wang, B.; Wang, C.; Wang, J.; Tian, Z.; Schlögl, R.; Su, D.S. Hydrothermal Carbon Enriched with Oxygenated Groups from Biomass Glucose as an Efficient Carbocatalyst. *Angew. Chem. Int. Ed.* **2017**, *56*, 600–604. [CrossRef] [PubMed]
112. Frusteri, L.; Cannilla, C.; Bonura, G.; Chuvilin, A.L.; Perathoner, S.; Centi, G.; Frusteri, F. Carbon microspheres preparation, graphitization and surface functionalization for glycerol etherification. *Catal. Today* **2016**, *277*, 68–77. [CrossRef]